Critical Mineral Characterization of the Tungsten Queen Mine Tailings, Vance County, North Carolina

Heather D. Hanna, Adam C. Curry, James S. Chapman, Dwain M. Veach, Katherine Pelt
North Carolina Geological Survey

North Carolina Geological Survey
Bulletin 100

February 2026

Suggested citation: Hanna, H.D., Curry, A.C., Chapman, J.S., Veach, D.M., and Pelt, K., 2026, Critical Mineral Characterization of the Tungsten Queen Mine Tailings, Vance County, North Carolina, North Carolina Geological Survey, Bulletin 100, 43 pages.

Contents

Key Findings

- The Tungsten Queen tailings impoundment contains an estimated 43,400,000 ft^3 of tailings.
- Resource estimates for the most enriched critical minerals in the impoundment are as follows:
    - Fluorine (66,695 metric ton [t] F, which is used as a proxy for fluorite/fluorspar)
    - Tungsten (2,706 t W; 3,413 t WO_3)
    - Manganese (1,732 t Mn)
    - Zinc (1,476 t Zn)
- Grainsize and/or density may have influenced lateral variations in critical mineral content of the tailings ponds.
- Heterogeneity of the ore being processed at a given time may have influenced depth-related variations in the critical mineral content of the tailings ponds.
- Compositional differences between tailings ponds 2 and 3 could suggest variability in the critical mineral content of certain minerals, including hubnerite, although the breakdown of certain sulfides could also be a factor.
- Acid-base accounting suggests kinetic testing is needed to determine the true potential for acid production from tailings, although data suggest two sulfide-rich samples are acid producing.

Abstract

The Tungsten Queen Mine, part of the Hamme Tungsten Mining District in northern Vance County, NC, produced over 900,000 t of WO_3, and minor quantities of Cu and Ag between 1942 and 1971. The Tungsten Queen tailings have been identified in previous investigations as a 'probable reserve' for W and a possible source for fluorite (fluorspar), galena, chalcopyrite, and high-purity quartz. This study presents the first comprehensive characterization of portions of the Tungsten Queen mine tailings for critical and non-critical mineral content.

Geochemical analyses of composite, grab, and drill core samples revealed inter-pond variability and lateral/vertical heterogeneity with possible implications for the relationship between grain size, mineral density, vein heterogeneity, and commodity distribution. Differences in the concentration of W with respect to Mn, and S with respect to Sb, As, and Te between tailings ponds 2 and 3 possibly reflect variations in mineral chemistry due to source heterogeneity, sulfide oxidation, and/or possible metal leaching. Using Li, Be, F, S, V, Mn, Zn, Ga, Ge, As, Rb, Y, Ag, Sb, Te, Cs, Dy, Er, Yb, W, Au, Pb, and Bi concentrations, principal component analysis (PCA) shows positive correlations between hubnerite elements W and Mn, sphalerite elements Zn and S, and the rare-earth elements (REE) Y, Dy, Er, and Yb. Volume analysis estimated 43.4 ft^3 of tailings, yielding approximately 2,706 t of W. Resource estimates for the critical minerals and non-critical commodities prioritized in this report range from 66,695 t for F to 8 t for Ge.

Acid-base accounting data provided a cursory assessment of the tailings' potential to produce acid. Net neutralization potential (NNP) and neutralization potential ratio (NPR) values for most Tungsten Queen samples fall within the range of uncertainty for one or both parameters, suggesting additional kinetic testing may be necessary for a more accurate evaluation. However, two sulfide mineral-rich samples plot in the net acid producing region for both NNP and NPR.

1. Introduction

Critical minerals are vital to the United States' economy and national security but are vulnerable to supply chain disruptions (e.g., Hofstra et al., 2021), necessitating efforts to identify potential domestic sources. This report uses the 2022 Critical Minerals list of the U.S. Geological Survey (U.S. Geological Survey, 2022). Mine waste, including that from some North Carolina mines, may be domestic sources that can help meet the country's critical mineral demand. However, existing data are not adequate to determine whether this potential exists for many mines, especially for critical minerals that were not the primary commodity. The USGS Earth Mapping and Resources Initiative (Earth MRI) funded this study to characterize the critical mineral content of the Tungsten Queen mine tailings as part of a nationwide effort to document the nature of critical mineral content in mine waste.

The Tungsten Queen mine is located in northern Vance County, North Carolina (Figure 1a) and is part of the ~2 km-wide, 13 km-long Hamme Tungsten Mining District, which follows a NNE trend from northern Vance County, North Carolina to Mecklenburg County, Virginia (Espenshade, 1945). The Tungsten Queen mine produced over 900,000 t of WO_3 while in operation between 1942 and 1971 (Foose et al., 1980) and is the only W mine east of the Rocky Mountains (Chaumba et al., 2015). The mine also previously produced minor amounts of copper (Cu) and silver (Ag) from sulfides (Chaumba et al., 2015). The Tungsten Queen tailings impoundment contains an estimated two million tons of tailings, which have been identified as a 'probable reserve' for W and may be a source for additional critical minerals based on the reported mineralogy of the deposit (Meyertons, 1975; Reid et al., 2017). Potential non-critical mineral commodities include galena, chalcopyrite, and high-purity quartz (Reid et al., 2017).

Tungsten Queen tailings show promise as a potential source for certain critical minerals; however, more detailed sampling is necessary to evaluate their concentration and distribution. Previous studies have focused primarily on tungsten or non-critical mineral commodities and did not examine the wider critical mineral content of the ponds. As such, published geochemical data for the tailings spans a limited range of analytes that exclude many critical minerals. This work is the first to characterize the Tungsten Queen tailings for additional critical minerals beyond W and to provide a full suite of publicly available compositional data. Evaluating the economic feasibility of processing the tailings for critical minerals is beyond the scope of this study. However, the geochemical data and interpretations could help inform future decisions regarding the presence of critical minerals and the potential for processing the Tungsten Queen mine waste.

Processing the Tungsten Queen mine tailings for critical minerals and other commodities could also help mitigate environmental contamination by utilizing minerals that could otherwise cause acid drainage or heavy metal contamination. For example, galena in the tailings is a possible source for Ag (Chaumba et al., 2015) but also poses a risk for Pb contamination. Thus, this study conducted a cursory assessment of the risk for acid production that could help inform environmental management for two local water supply reservoirs.

2. Geologic Setting, Mining History, and Prior Work

The Hamme Tungsten Mining District is part of the Carolina terrane, which is a Neoproterozoic to Cambrian volcanic island arc that formed off the coast of Gondwana (Hibbard et al., 2002, 2006). Three lithotectonic units comprise the Carolina terrane. The oldest is the ca. 633 to 612 Ma Hyco Arc (Wortman et al., 2000; Bowman, 2010; Bradley and Miller, 2011), interpreted as a mature arc built on oceanic lithosphere (Hibbard et al., 2013). An approximately 37 million year disconformity separates the Hyco Arc from the overlying redefined Virgilina sequence of Bowman et al. (2013). The redefined Virgilina sequence is composed of the mostly

metasedimentary Aaron Formation, which has youngest detrital zircon ages of 588 Ma (Pollock et al., 2010) and 578 Ma (Sampson et al., 2001), and the metavolcanic Virgilina member of the Aaron Formation (Bowman et al., 2013; Hibbard et al., 2013). The youngest lithotectonic unit is the ca. 555 to <528 Ma Albermarle arc (Hibbard et al., 2013), which is built on a basement that includes a continental component (Mueller et al., 1996). The Carolina terrane is composed of low-grade meta-igneous, metavolcano-sedimentary, and metasedimentary rocks (Secor et al., 1983; Hibbard et al., 2002, 2006). In the eastern part of the field area, granodiorite of the Vance County pluton was emplaced in the late Neoproterozoic, ca. 571 Ma (Fig. 1; LeHuray, 1989).

Tungsten was exploited from hubnerite-bearing quartz veins (Gair et al., 1975), which were deposited as a skarn-replacement-vein W deposit which formed in a porphyry Cu-Mo-Au mineral system (Hofstra and Kreiner, 2020; Hammarstrom et al., 2022). The lenticular to tabular hubnerite-bearing veins are hosted in granodiorite of the Neoproterozoic Vance County pluton and to a lesser extent in adjacent phyllitic rock of the Aaron Formation (Espenshade, 1945; Parker, 1963; Horton et al., 2022); Figure 1). Approximately 50 of the ~90 mapped quartz veins contain hubnerite (Chaumba et al., 2015 and references therein), and the granodiorite-hosted veins have more mineralization than those hosted in the phyllite (Espenshade, 1945). The veins are hydrothermal in origin and subsequently underwent amphibolite facies-grade metamorphism (Foose and Slack, 1978; Casadevall and Rye, 1980). Horton et.al. (2022) proposed that the veins are of Mississippian age (ca. 358.9 - 323.2 Ma) and were metamorphosed to amphibolite grade conditions during the Alleghenian Orogeny (320-280 ma), but they also acknowledge that a significant, older metamorphic event also occurred in this region of the Carolina Terrane. The most hubnerite-rich veins are concentrated in an ~3 km-long, 0.5 km-wide zone in the central portion of the district, with the most important being the Tungsten Queen vein ((Espenshade, 1945; Feiss et al., 1991). The Tungsten Queen vein is ~3,000 m long and ranges from <1 m to 10 m wide, striking N35E and dipping eastward at 70 to 90^{o} (Casadevall and Rye, 1980). The most abundant minerals in the vein are quartz (92%), sericite (3%), fluorite (1%), hubnerite (<0.5%), and pyrite (<0.5%; Casadevall and Rye, 1980). Additional minerals reported in trace quantities are listed in Table 1. Hubnerite is the principal tungsten ore, although scheelite is also present in quantities of <0.1% (e.g., Casadevall and Rye, 1980).

Tungsten minerals were discovered in what would become the Hamme Tungsten Mining District by brothers Joseph and Richard Hamme in 1942 (U.S. Department of Interior Bureau of Mines, 1944; Espenshade, 1945; Meyertons, 1975). The Hamme brothers mined some veins using shallow pits and shafts until August 1943 when Haile Mines, Inc. acquired the property and began large scale mining (Espenshade, 1945). In June 1945, Haile Mines, Inc., joined with General Electric Co. to form Tungsten Mining Corp., and the operations produced a combined 21,457 t of WO_3 from May 1943 to March 1946 (Espenshade, 1945). Mining continued until market fluctuations forced the mine to close from June 30, 1958, to June 1, 1960, then closed again from early 1963 to 1968 (North Carolina Department of Natural and Cultural Resources, 2023). Ranchers Exploration Company acquired the mine in 1968 and renamed it Tungsten Queen (Meyertons, 1975). The Tungsten Queen was in operation until declining WO_3 prices led to its final closure in August 1971 (Meyertons, 1975). Operations over the life of the mine left a tailings impoundment composed of three tailings ponds (Figure 2). Tailings ponds 1 and 2 and a portion of tailings pond 3 are currently located on land owned by Townsville Timber, Inc., while most of tailings pond 3 is on property owned by the United States Army Corps of Engineers

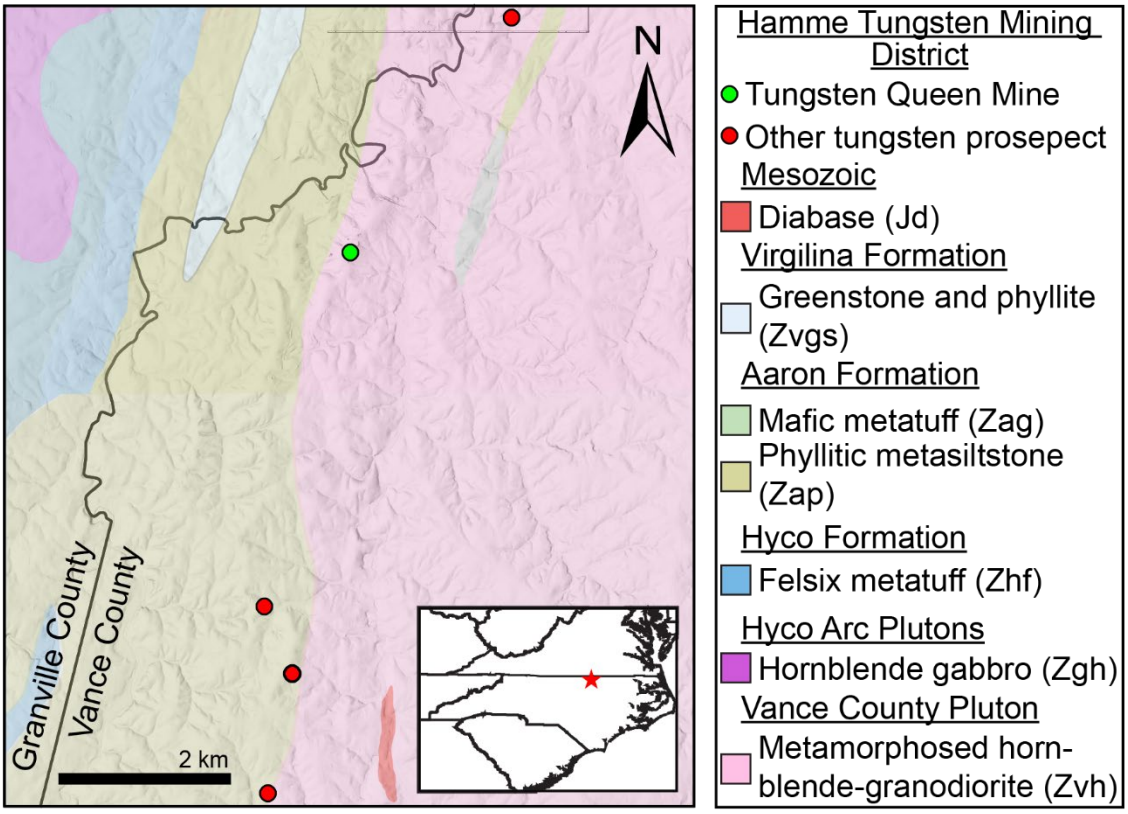

Figure 1. Map of Tungsten Queen Mine in norther Vance County, NC, near the border with Granville County to the west. Inset map shows location of mine near the border with Virginia. Geology is from Horton et al. (2022) and Blake et al. (2025) and overlies a hillshade built from a 3-ft resolution DEM.

(USACE; Figure 2). Tailings ponds 2 and 3 are separated by a dam constructed on top of existing tailings by the mine operators in 1970.

The Tungsten Queen deposit has been the subject of multiple studies (U.S. Department of Interior Bureau of Mines, 1944; Espenshade, 1945; Parker, 1963; Gair et al., 1975; Gair, 1977; Foose and Slack, 1978; Casadevall and Rye, 1980; Foose et al., 1980, 1981; Chaumba et al., 2015; Parker et al., 2015), however, publicly-available work on the Tungsten Queen tailings is more limited and has primarily focused on W, galena, and quartz (Meyertons, 1975; Chaumba et al., 2015; Parker et al., 2015; Reid et al., 2017). Meyertons (1975) concluded the Tungsten Queen tailings are a 'probable reserve' of W, with 2,038,000 t of tailings containing a total of 404,242 t $W0_3$. Note that Meyertons (1975) does not specify whether this 2,038,000 is metric tons (t) or short ton units (STU), but given his use of STU throughout the publication, we assume it to be STU. Reid et al. (2017) evaluated the Tungsten Queen mine tailings as a source of high-purity quartz, concluding it could be suitable for silica glass and fused quartz applications. Reid et al. (2017) also noted that fluorite represents up to 2.5 weight percent (wt%) of the heavy fraction, with potentially recoverable hubnerite, scheelite, galena, chalcopyrite, and sphalerite as accessory minerals. Chaumba et al. (2015) and Parker et al. (2015) conducted electron microprobe analysis on hubnerite-wolframite in Tungsten Queen ore and tailings samples and concluded they were highly enriched in the critical mineral manganese. The microprobe studies also provided information on the chemistry of Tungsten Queen chalcopyrite and galena; however, the work focused on constraining the deposit's geologic environment of formation

Table 1. Deposit Mineralogy, Critical Minerals, and Estimated Mineral Abundance

Mineral Reported in Vein	Chemical Formula	Critical Minerals[4]	Estimated Mineral Abundance in Vein[1]
Quartz[1]	SiO_2	N/A	92%
Sericite[1]	$KAl_3Si_3O_{10}(OH,F)_2$	Al	3%
Fluorite[1]	CaF_2	Fluorite	1%
Hubnerite[1]	$MnWO_4$	Mn, W	<0.5%
Pyrite[1]	FeS_2	N/A	<0.5%
Chalcopyrite[1]	$CuFeS_2$	N/A	<0.1%
Sphalerite[1]	ZnS	Zn	<0.1%
Galena[1]	PbS	N/A	<0.1%
Bornite[1]	Cu_5FeS_4	N/A	<0.1%
Molybdenite[1]	MoS_2	N/A	<0.1%
Chalcocite[1]	CuS_2	N/A	<0.1%
Scheelite[1]	$CaWO_4$	W	<0.1%
Tetrahedrite[1]	$(Cu,Fe,Zn)_{12}Sb_4S_{13}$	Sb	<0.1%
Beryl[1]	$Be_3Al2Si_6O_{18}$	Be, Al	<0.1%
Rhodochrosite[1]	$MnCO_3$	Mn	<0.1%
Calcite[1]	$CaCO_3$	N/A	<0.1%
Ankerite[1]	$Ca(Fe,Mg,Mn)(CO_3)_2$	Mn, Mg	<0.1%
Apatite[1]	$Ca_5(PO_4)_3(F,Cl,OH)$	N/A	<0.1%
Dolomite[2]	$CaMg(CO_3)_2$	Mg	not given
Gold[2]	Au	N/A	not given
Topaz[2]	$Al_2SiO_4(F,OH)_2$	Al	not given
Garnet (Spessartine?)[2]	$Mn_3Al_2SiO_4$	Mn	~0.1%[5]
Altaite[3]	PbTe	Te	<0.1%
Wittichenite[3]	BiS	Bi	<0.1%
Volynskite[3]	$AgBiTe_2$	Bi, Te	<0.1%

[1]Hydrothermal minerals of Casadevall and Rye (1980)
[2]Foose (1980) and references therein
[3]Reported as present or potentially present in unpublished notes from J.F. Slack in 1977 as reported by Foose (1980)
[4]USGS 2022 critical minerals list (U.S. Geological Survey, 2022)
[5]Espenshade (1947) reports ~0.1% garnet was identified in the tailings by E.S. Larson. All other mineral percentages are from Casadevall and Rye (1980) for the hydrothermal minerals in the Tungsten Queen Snead-Walker vein.

(Chaumba et al., 2015) and comparing it to other hubnerite deposits (Parker et al., 2015) instead of characterizing critical mineral content of the tailings.

3. Methods

Three types of samples were collected from the Townsville Timber, Inc., portion of the tailings ponds where the North Carolina Geological Survey (NCGS) staff had permission to access. Composite samples were collected according to Earth MRI Mine Waste grant protocol (U.S. Geological Survey, 2023). The tailings ponds were divided into composite sample units based on variations in surface tailings color and/or variations in tailings pond elevations (Figure 2). A minimum of thirty subsample locations were identified for each composite sample unit and marked in the field with stakes. NCGS staff dug an initial test pit for each composite sample unit to determine a subsampling depth that would avoid light-colored surficial tailings that could be affected by surface alteration. In some composite sample units, a subsampling depth was selected

that balanced the need to avoid surface contamination with thickness considerations in areas with very thin tailings cover. Subsampling depths ranged from 1 to 4 inches depending on the composite sample unit, and all subsamples for a given composite sample were collected from the same depth.

NCGS staff systematically collected each subsample by removing overlying tailings until the target depth was reached, then scooping a tailings subsample to the 4 inch mark on the stainless-steel trowel. Each subsample was then sieved into a bucket using a 2 mm sieve. The <2 mm fraction for each subsample was collected in the bucket with the other subsamples while the >2 mm fraction was discarded. When all subsamples had been collected in the bucket, the bucket was secured with a lid and labeled with the composite sample number. Composite samples were then taken back to the lab at the NCGS Coastal Plain Office and Core Repository, dried, and described before ~1 to 2 kilograms (kg) of sample was sent to USGS Sample Control (Denver, CO) for analysis. Field sheets for composite samples are given in Appendix 1.

Grab samples were collected from areas of scientific interest (Figure 2) using a clean stainless-steel trowel and placed in a sample bag without sieving. At least 1 kg of sample was

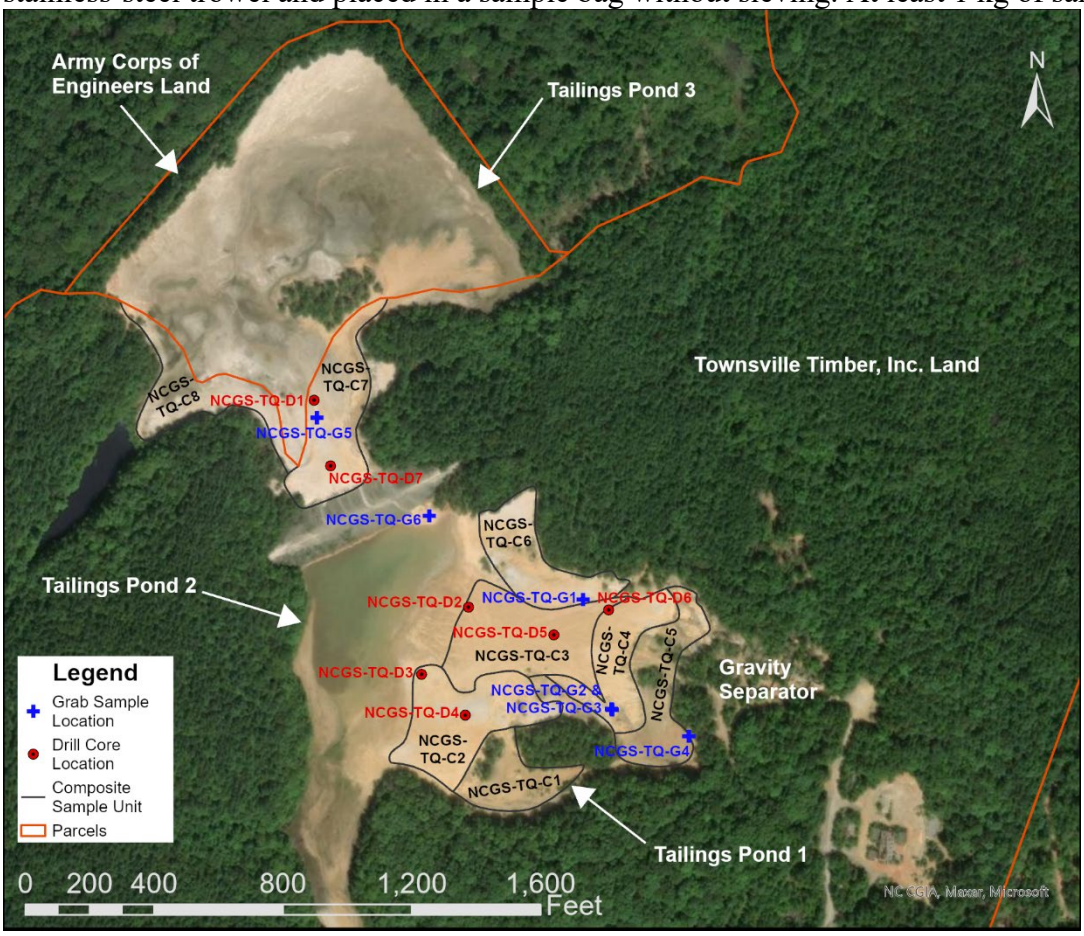

Figure 2. Map of Tungsten Queen tailings impoundment showing location of tailings ponds, parcel boundaries, sample, and the gravity separator. Composite sample units are delineated by black lines and identified with black labels, grab samples labels are in blue, and sonic core labels are in red. Island Creek follows the USACE property line immediately north of tailings pond 3.

collected whenever possible. Grab samples from most locations were collected from features of interest within 4 inches of the surface, however, grab samples were also collected from two vertical profiles exposed along an erosional bank in the tailings (NCGS-TQ-G2 and NCGS-TQ-

G3 on Figure 2). Surface tailings were scraped from profiles using a stainless-steel trowel to expose fresh tailings, then vertical sample boundaries were delineated according to changes in lithology and/or tailings color within each profile. Samples were then collected spanning the full vertical extent delineated for each sample to give an average composition for that interval of the profile. Samples were deposited into resealable plastic bags labeled with the grab sample profile number and depth interval. Samples were taken back to the lab, dried, described, and sent to USGS Sample Control for analysis. Grab sample field sheets are available in Appendix 1.

Seven 4-inch diameter drill cores were collected using a sonic drill rig (Figure 2). Each run was extruded from the core barrel into plastic sleeves which were then placed into labeled wooden core boxes. The core boxes were taken back to the lab, the plastic sleeves were opened, and the cores were partially dried since some runs contained significant excess water. The cores were then photographed (Appendix 2) and sampled in 1 ft intervals avoiding material near the edges to minimize risk of contamination. Approximately 1.2 kg of material was collected in a continuous channel for the full 1 ft interval. When the core recovered in a run did not end on an even foot mark, the remaining interval was collected as a separate sample if it was ~0.7 ft or greater, and was included with the previous 1 ft interval if it was <0.7 ft. The 0.7 ft mark was chosen as the lower cutoff for a separate sample because of the need for enough material to collect an ~1.2 kg sample while still retaining an archive portion of the core. Core samples were sieved using a 2 mm sieve, dried if needed, described, and sent to USGS Sample Control for analysis. Field sheets for drill cores are given in Appendix 1.

All sample processing (drying, description, etc.) was conducted in the lab at the NCGS Coastal Plain Office before submission to the USGS. As per the sampling protocol, one out of every 10 composite, grab, and core samples collected was a duplicate. Upon receipt, the USGS facilitated additional sample prep and submission of samples to a laboratory for chemical analysis. Major elements were acquired using x-ray fluorescence (XRF), and trace elements were acquired using inductively-coupled plasma optical emission spectroscopy (ICP-OES) The resulting sample data underwent QA/QC by the USGS to establish which elements met USGS data quality standards while flagging those that did not. Spreadsheets were then sent to NCGS scientists who removed elements flagged by the USGS and averaged data for duplicated samples. Samples with averaged duplicate concentrations are reported with an * at the end of the sample number in Appendix 3 with the number of duplicates included in the average noted in the "Sample Description" column. Sample numbers follow the format NCGS-TQ-<sample type><sample number>, where NCGS stands for North Carolina Geological Survey, TQ stands for Tungsten Queen, the sample type is composite (C), grab (G), or drill core (D), and the sample number is 1, 2, 3, etc. Drill cores and the two grab sample profiles also have the depth interval after the sample number as start depth-end depth (in inches for grab samples and feet for cores). For example, composite sample 1 is noted in Appendix 3 as NCGS-TQ-C1; the 0 to 4 in interval of grab sample profile 2 would be NCGS-TQ-G2-0-4; and the 16 to 17.2 ft interval of core 2 would be NCGS-TQ-D2-16-17.2.

4. Results

One goal of this study was to characterize the potential in the mine tailings for enrichment of critical minerals other than tungsten, which was previously mined from hubnerite. To evaluate which critical minerals to include in the report, this study used published information on Tungsten Queen vein mineralogy to determine which minerals may be present in the tailings and what critical minerals are included in their chemical formulas (Table 1). Critical minerals Sb, Be, Bi, Mn, Te, W, and Zn were selected for inclusion because they are major

components in the reported mineralogy. The critical minerals Al, a major component in some of the reported silicate minerals, and Mg, a major component in dolomite and ankerite, were not included due to very low concentrations given they are otherwise abundant in the Earth's crust. Finally, F is included as a proxy for the critical mineral fluorspar (fluorite) in geochemical diagrams since fluorite is the primary fluorine-containing mineral reported for the Tungsten Queen vein. However, F is not a perfect proxy since it could also occur in small amounts in apatite and topaz (Table 1).

Some critical minerals are not major components in reported Tungsten Queen vein minerals but can incorporate into certain minerals in potentially meaningful quantities. Arsenic (As) is included in this report because it can commonly be present in pyrite, and in addition to being a critical mineral, As in sulfides has been implicated as a source for As in groundwater in other areas of the Carolina terrane (Abraham, 2009; Dinwiddie and Liu, 2018). Critical minerals Ga and Ge can substitute into sphalerite (Foley et al., 2017; Gnesda et al., 2020, respectively), and at the time of the writing of this report, are subject to export restrictions that Nassar et al. (2024) estimate could have a $3.4 billion impact on the United States economy. Finally, vanadium (V) was included, which positive co-variations on geochemical plots suggest may be substituting for Al or present in Al-bearing minerals.

Silver and Au, while not critical minerals, are included in this report because of the economic importance of both commodities, and the potential for Ag production from Tungsten Queen galena as a byproduct of WO_3 mining (Chaumba et al., 2015; Parker et al., 2015). The full list of critical minerals and non-critical commodities featured in this report are listed in Table 2 along with their chemical symbols (abbreviations). All geochemical data collected for Tungsten Queen samples, including elements not discussed in this report, are available in Appendix 3. Appendix 3 also includes samples NCGS-TQ-D1-24-25, NCGS-TQ-D1-25-26.9, NCGS-TQ-D1-30-31.8, NCGS-TQ-D1-32-34.3, NCGS-TQ-G4, and NCGS-TQ-C1. Geochemical data from these samples were not discussed in this report because sample texture and chemistry (e.g., low silicon, high loss on ignition, very high Al and iron) indicated their chemical compositions

Table 2. List of Critical Minerals and Non-Critical Commodities Highlighted in this Report and their Chemical Symbols

Critical Mineral	Chemical Symbol
Antimony	Sb
Arsenic	As
Beryllium	Be
Bismuth	Bi
Fluorine*	F
Gallium	Ga
Germanium	Ge
Manganese	Mn
Tellurium	Te
Tungsten	W
Vanadium	V
Zinc	Zn
Non-Critical Commodity	**Chemical Symbol**
Gold	Au
Silver	Ag

*Used as a proxy for the critical mineral, fluorspar

reflected regolith instead of tailings. For NCGS-TQ-C1, this aligns with reports that the tailings had been previously moved out of the pond.

4.1 Critical Minerals

Fluorine (Proxy for Fluorite/Fluorspar)

Concentrations of F in composite samples range from 1.082 to 1.8957 wt% (Figure 3a), with a mean of 1.5856 wt% and a median of 1.6744 wt%. The highest concentrations are in NCGS-TQ-C6 (1.8957 wt%), located in the northeastern portion of tailings pond 2, and NCGS-TQ-C7 (1.8882 wt%), located in the southern portion of tailings pond 3 (Figure 3b).

Grab sample F concentrations range from 0.9029 to 2.3449 wt%, although most samples fall within the same range as the composite samples. The mean concentration is 1.4251 wt% while the median is 1.2571 wt%. Samples NCGS-TQ-G3-28-30 (2.3449 wt%) and NCGS-TQ-G2-0-4 (2.0114 wt%) contain the highest grab sample F concentrations (Figure 3a).

Drill cores span the widest compositional range, from 0.9006 to 9.3162 wt% F, and have a mean value of 2.6910 wt% and a median of 2.1291 wt% (Figure 4). The highest core sample

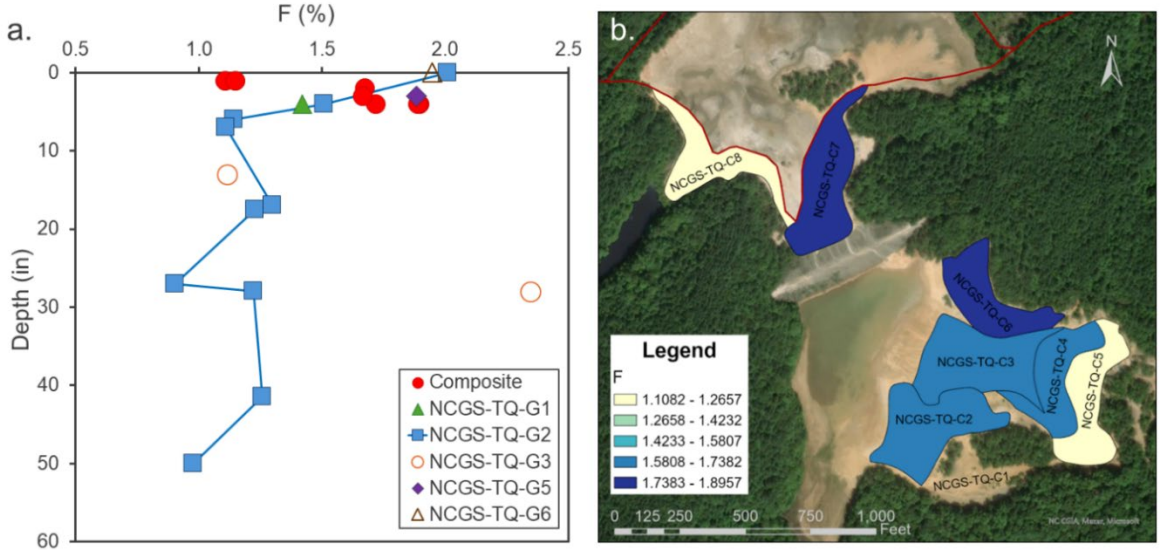

Figure 3. a. F concentration versus depth for composite and grab samples. b. Heat map for F concentration (wt%) in composite samples. Darkest blue represents the highest values with yellow representing the lowest. See text for more information.

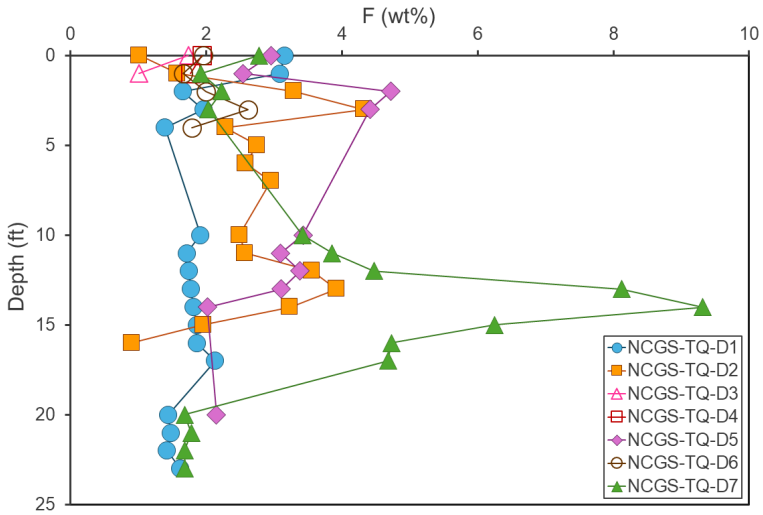

Figure 4. F concentration versus depth for Tungsten Queen Cores. See text for more information.

concentrations are in NCGS-TQ-D7-14-15 (9.3162 wt%) and NCGS-TQ-D7-13-14 (8.1188 wt%), with NCGS-TQ-D7-15-16 also containing elevated F (6.2500 wt%; Figure 4).

Tungsten

Concentrations of W in composite samples range from 459 to 1330 parts per million (ppm; Figure 5a), with a mean of 955 ppm and a median of 962 ppm. The highest concentrations are in NCGS-TQ-C3 (1330 ppm) and NCGS-TQ-C6 (1240 ppm), located in the central and northeastern portions of tailings pond 2, respectively (Figure 5b).

Tungsten concentrations in grab samples range from 289 to 2400 ppm, with a mean value of 825 ppm and a median value of 533 ppm. The highest grab sample W concentrations are in samples NCGS-TQ-G3-28-30 (2400 ppm) and NCGS-TQ-G2-0-4 (1770 ppm; Figure 5a).

Drill cores range from 366 to 3310 ppm, with a mean W content of 825 ppm and a median of 533 ppm (Figure 6). Highest concentrations are recorded in NCGS-TQ-D5-0-1 (3310

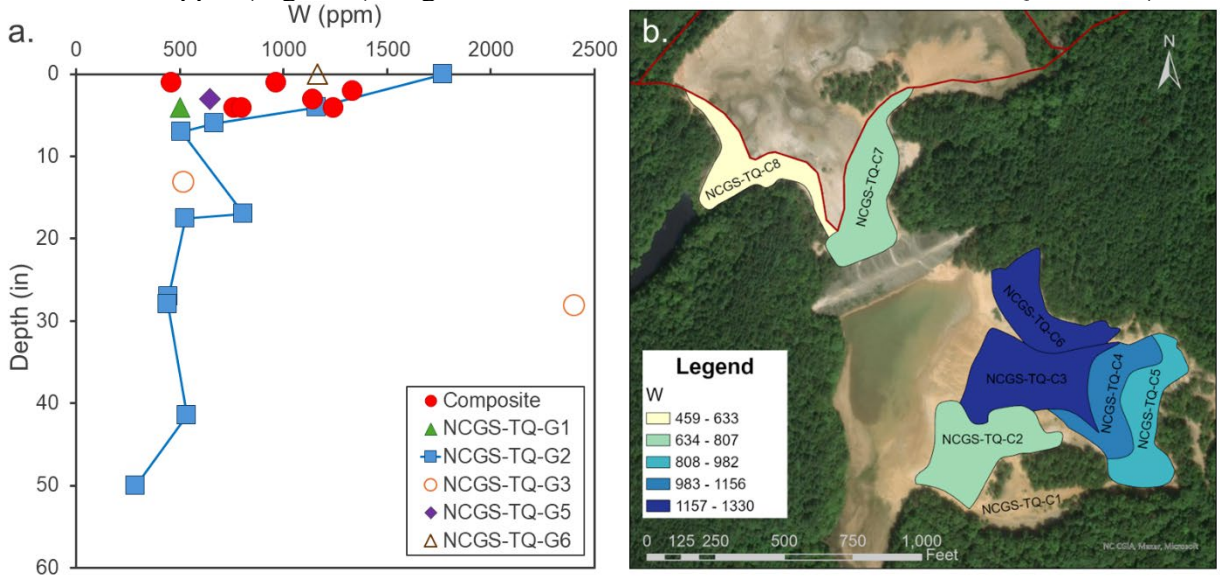

Figure 5. a. W concentration versus depth for composite and grab samples. b. Heat map for W concentration (ppm) in composite samples. Darkest blue represents the highest values with yellow representing the lowest. See text for more information.

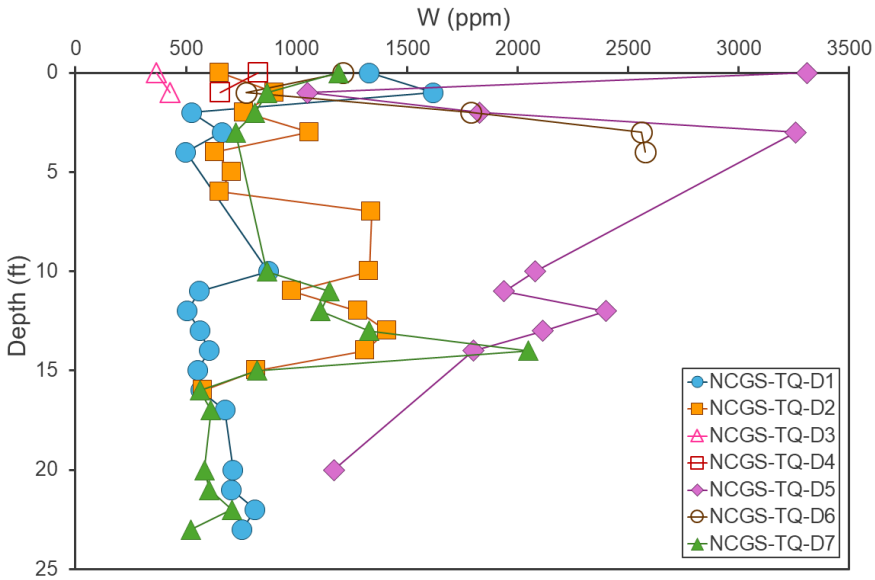

Figure 6. W concentration versus depth for Tungsten Queen Cores. See text for more information.

ppm) and NCGS-TQ-D5-3-4.4 (3260 ppm), with additional notable W spikes in NCGS-TQ-D6-3-4 (2560 ppm), NCGS-TQ-D6-4-4.7 (2580 ppm), and NCGS-TQ-D5-12-13 (2400 ppm; Figure 6).

Manganese

Composite sample Mn concentrations range from 502 to 695 ppm (Figure 7a), with the highest concentrations in NCGS-TQ-C5 and NCGS-TQ-C6, located in the eastern and northeastern portions of tailings pond 2, respectively (Figure 7b). The mean Mn concentration is 609 ppm while the median is 653 ppm.

Grab sample Mn concentrations range from 232 to 1885 ppm, with a mean of 656 ppm and a median of 380 ppm. The highest grab sample Mn concentrations are in NCGS-TQ-G1 (1860 ppm) and NCGS-TQ-G5 (1885 ppm; Figure 7a).

Drill cores range from 298 to 2020 ppm, with a mean of 709 ppm and a median of 636 ppm. The highest concentrations are in NCGS-TQ-D7-14-15 (2020 pm) and NCGS-TQ-D6-4-4.7 (1910 ppm; Figure 8).

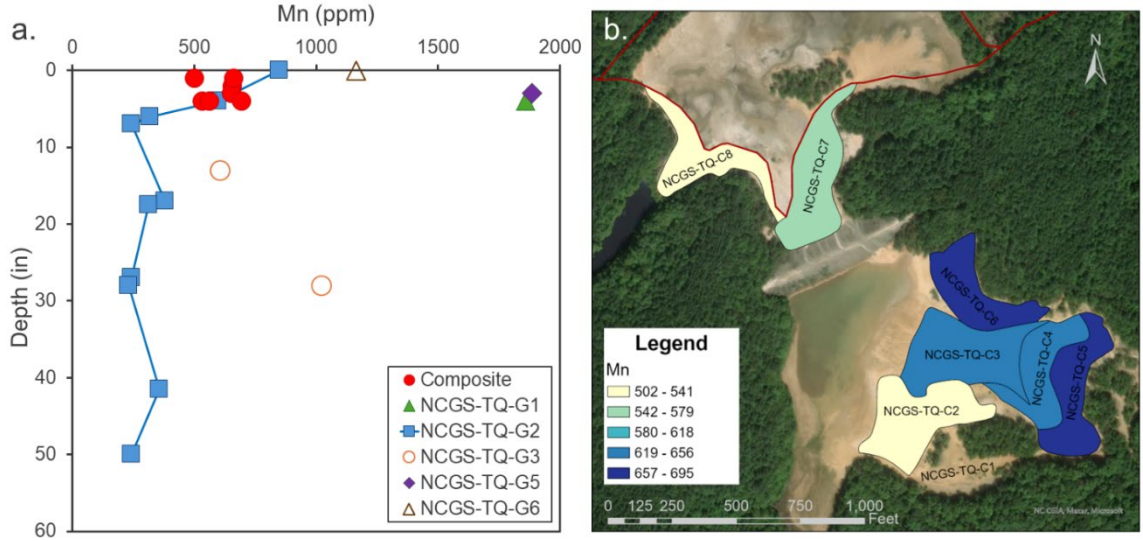

Figure 7. a. Mn concentration versus depth for composite and grab samples. b. Heat map for Mn concentration (ppm) in composite samples. Darkest blue represents the highest values with yellow representing the lowest. See text for more information.

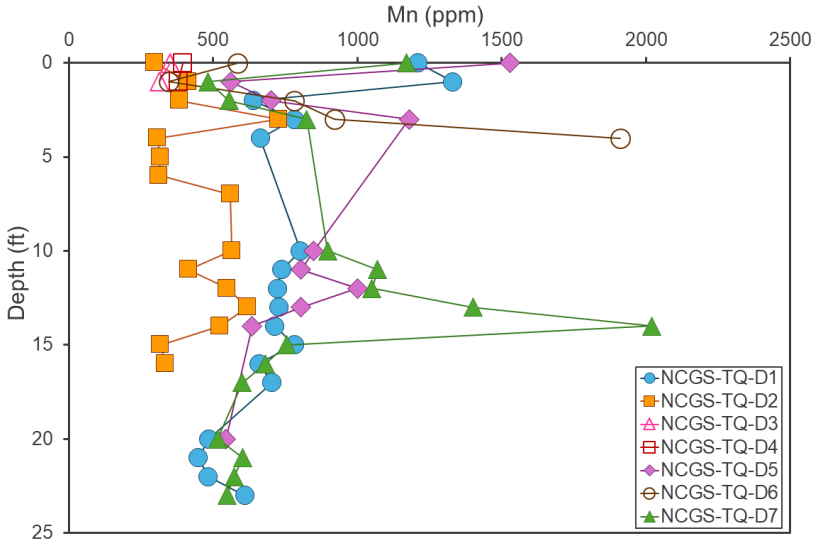

Figure 8. Mn concentration versus depth for Tungsten Queen Cores. See text for more information.

Zinc

Composite sample Zn concentrations range from 208 to 864 ppm (Figure 9a), with the highest concentration in NCGS-TQ-C3, located in the central portion of tailings pond 2 (Figure 9b). The mean concentration is 456 ppm with a median of 345 ppm.

Grab sample Zn concentrations range from 84 to 1120 ppm, though all but one sample fall between 84 to 507 ppm (Figure 9a). The mean Zn concentration for grab samples is 244 ppm with a median of 137 ppm. The highest grab sample concentrations are in samples NCGS-TQ-G1 (1120 ppm) and NCGS-TQ-G3-28-30 (507 ppm; Figure 9a).

Drill cores range from 81 to 1850 ppm Zn, with a mean of 600 ppm and a median of 499 ppm. The highest concentrations are in NCGS-TQ-D7-14-15 (1850 ppm) and NCGS-TQ-D1-1-2 (1815 ppm; Figure 10).

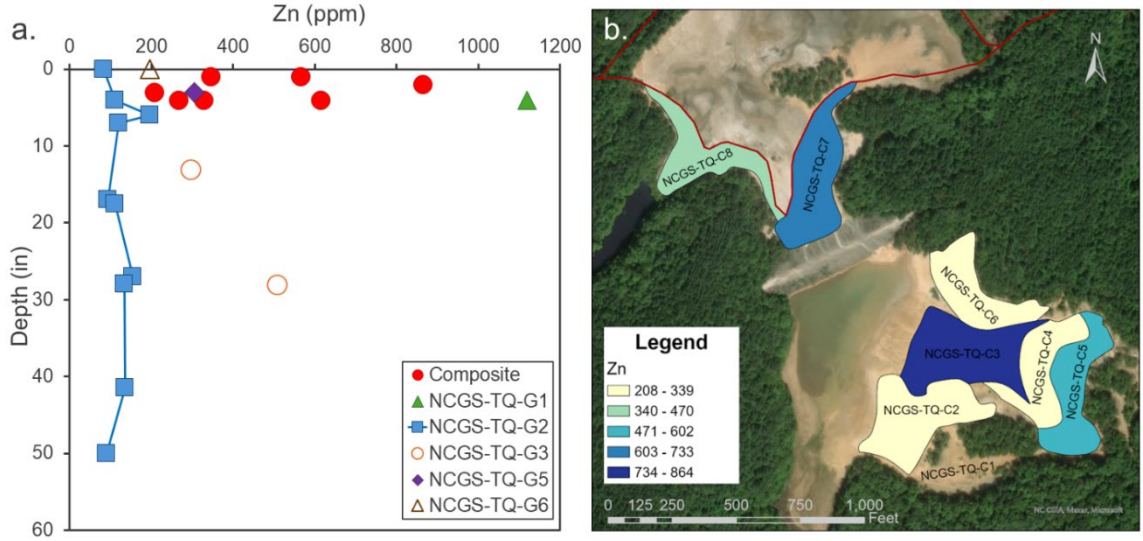

Figure 9. a. Zn concentration versus depth for composite and grab samples. b. Heat map for Zn concentration (ppm) in composite samples. Darkest blue represents the highest values with yellow representing the lowest. See text for more information.

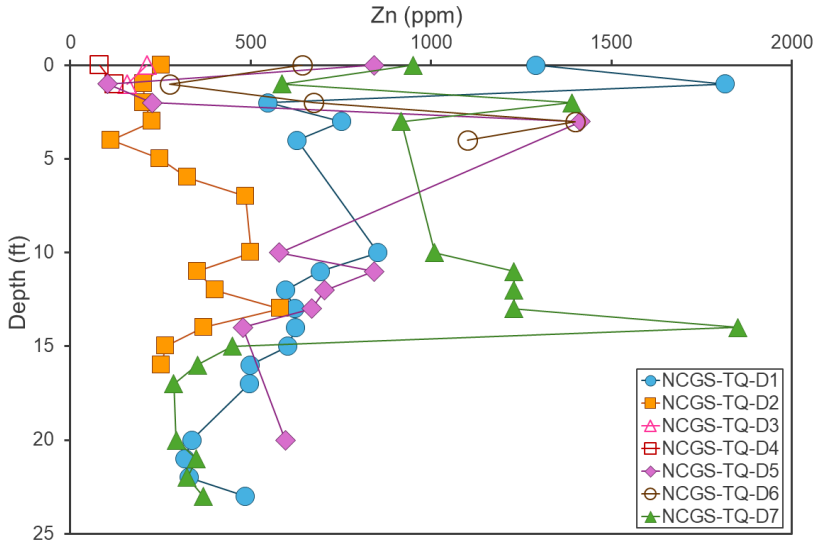

Figure 10. Zn concentration versus depth for Tungsten Queen Cores. See text for more information

Antimony

Composite sample Sb concentrations range from 54 to 184 ppm (Figure 11a), with the highest concentration in NCGS-TQ-C5, located in the eastern portion of tailings pond 2 (Figure 11b). The mean Sb value for composite samples is 113 ppm while the median is 120 ppm.

Grab sample Sb concentrations range from 55 to 220 ppm, though most samples fall from 55 to 110 ppm (Figure 11a). The mean concentration is 93 ppm, and the median is 77 ppm. The highest grab sample Sb concentrations are in NCGS-TQ-G3-28-30 (220 ppm) and NCGS-TQ-G2-6-7 (151 ppm; Figure 11a).

Drill core Sb concentrations range from 20 to 354 ppm, with a mean of 99 ppm and a median of 86 ppm. The highest concentrations are in NCGS-TQ-D5-3-4.4 (354 ppm) and NCGS-TQ-D6-3-4 (275 pm Figure 12).

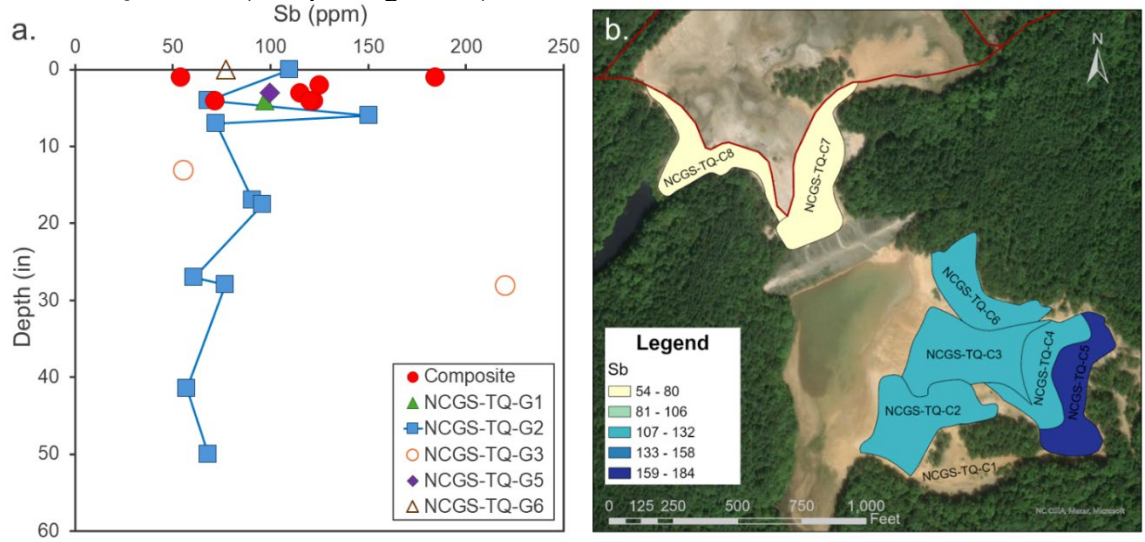

Figure 11. a. Sb concentration versus depth for composite and grab samples. b. Heat map for Sb concentration (ppm) in composite samples. Darkest blue represents the highest values with yellow representing the lowest. See text for more information.

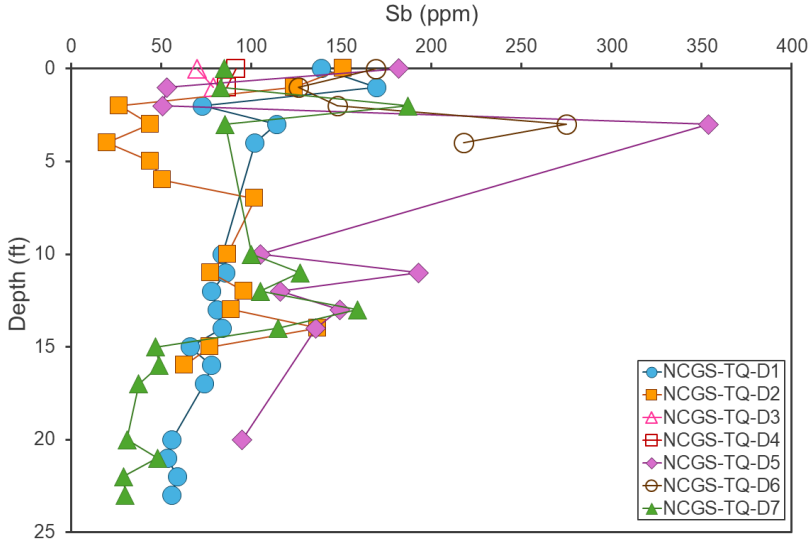

Figure 12. Sb concentration versus depth for Tungsten Queen Cores. See text for more information.

Arsenic

Composite sample As concentrations range from 21 to 73 ppm (Figure 13a), with the highest concentrations in NCGS-TQ-C5, located in the eastern portion of tailings pond 2 (Figure 13b). The mean concentration for composite samples is 43 ppm and the median concentration is 44 ppm.

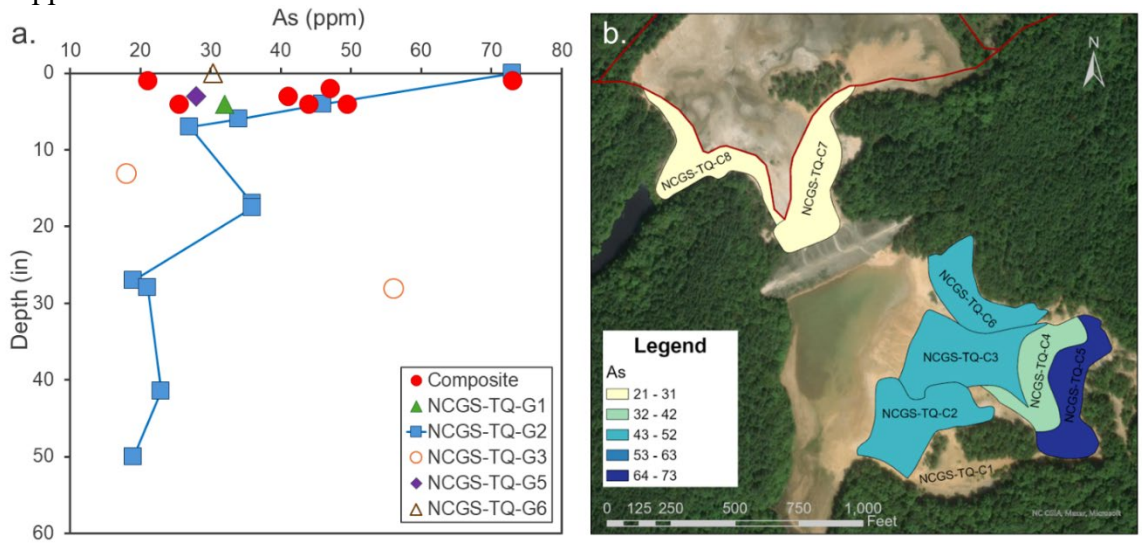

Figure 13. a. As concentration versus depth for composite and grab samples. b. Heat map for As concentration (ppm) in composite samples. Darkest blue represents the highest values with yellow representing the lowest. See text for more information.

Grab sample As concentrations range from 18 to 73 ppm, spanning a similar range as the composite samples (Figure 13a). The mean As concentration is 33 ppm while the median was 30 ppm. The highest grab sample As concentrations are from NCGS-TQ-G2-0-4 (73 ppm) and NCGS-TQ-G3-28-30 (56 ppm; Figure 13a).

Four drill cores have As concentrations below the 10 ppm detection limit (NCGS-TQ-D2-2-3, NCGS-TQ-D2-4-5, NCGS-TQ-D7-20-21, and NCGS-TQ-D7-22-23Ave), while the rest range from 10 to 131 ppm with a mean of 40 ppm and a median of 36 ppm (Figure 14). The

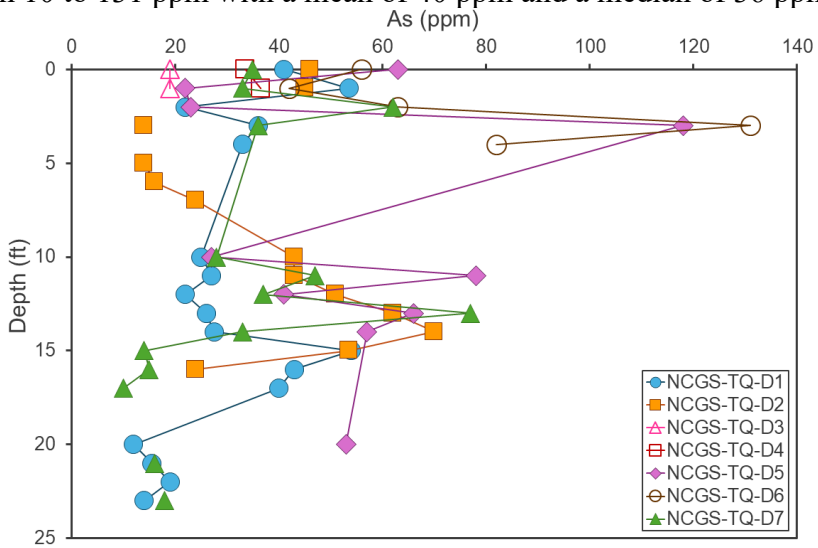

Figure 14. As concentration versus depth for Tungsten Queen Cores. See text for more information.

highest As concentrations are in samples NCGS-TQ-D6-3-4 (131 pm) and NCGS-TQ-D5-3-4.4 (118 ppm; Figure 14).

Tellurium

Composite sample Te concentrations range from 11.1 to 31.0 ppm (Figure 15a), with the highest concentrations in NCGS-TQ-C5, located in the eastern portion of tailings pond 2 (Figure 15b). The mean and median composite sample Te concentrations are both 19 ppm.

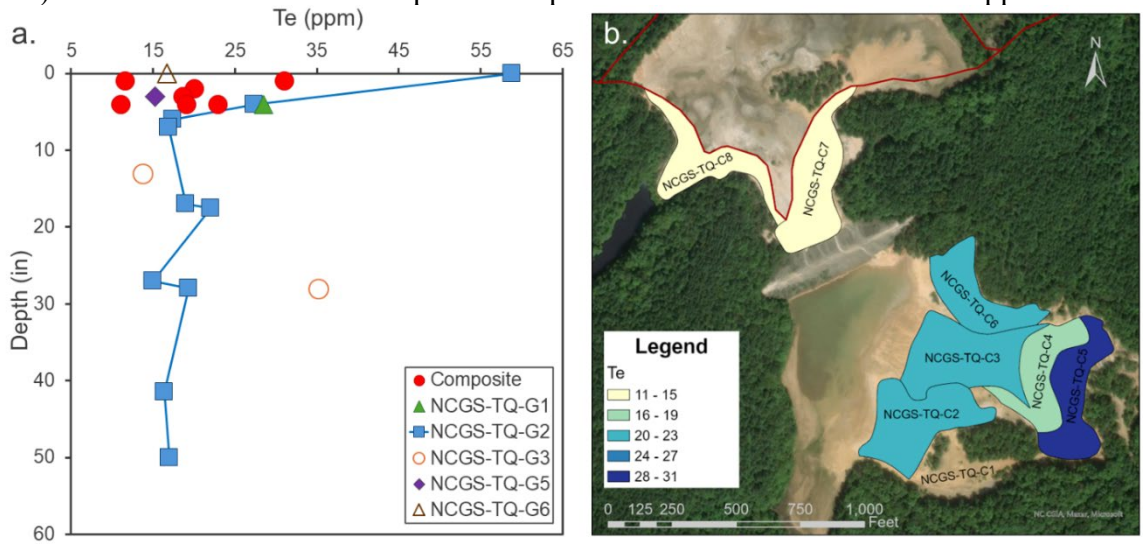

Figure 15. a. Te concentration versus depth for composite and grab samples. b. Heat map for Te concentration (ppm) in composite samples. Darkest blue represents the highest values with yellow representing the lowest. See text for more information.

Grab sample Te concentrations range from 13.7 to 58.8 ppm, although only one sample has a concentration >36 ppm (Figure 15a). The mean concentration is 23 ppm with a median of 17 ppm. The highest grab sample Te concentrations are in NCGS-TQ-G2-0-4 (58.8 ppm) and NCGS-TQ-G3-28-30 (35.2 ppm; Figure 15a).

Drill cores range from 12.8 to 69.9 ppm Te, with a mean of 24 ppm and a median of 22 ppm. The highest Te concentrations are in NCGS-TQ-D5-3-4.4 (69.9 ppm), NCGS-TQ-D2-6-7 (66.0 ppm), and NCGS-TQ-D6-3-4 (62.7 pm; Figure 16).

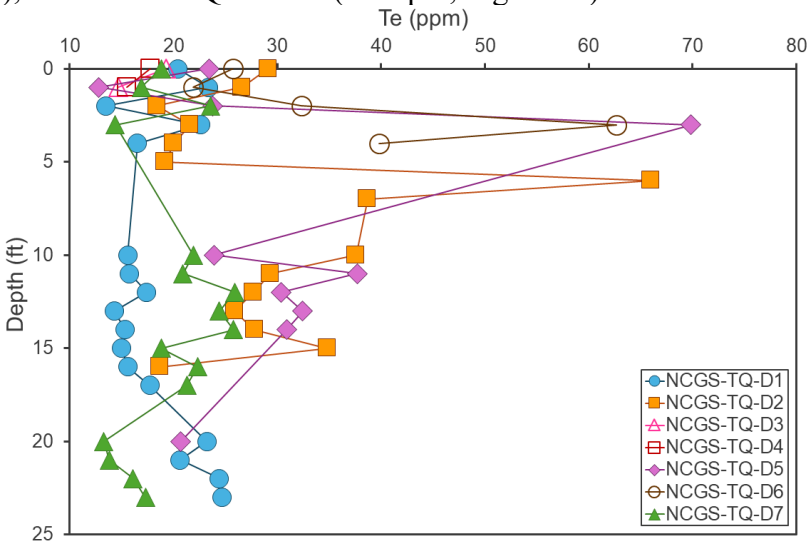

Figure 16. Te concentration versus depth for Tungsten Queen Cores. See text for more information.

Vanadium

Composite sample V concentrations range from 20 to 55 ppm (Figure 17a), with a mean of 28 ppm and a median of 25 ppm. The highest concentration is in NCGS-TQ-C5, located in the eastern portion of tailings pond 2 (Figure 17b).

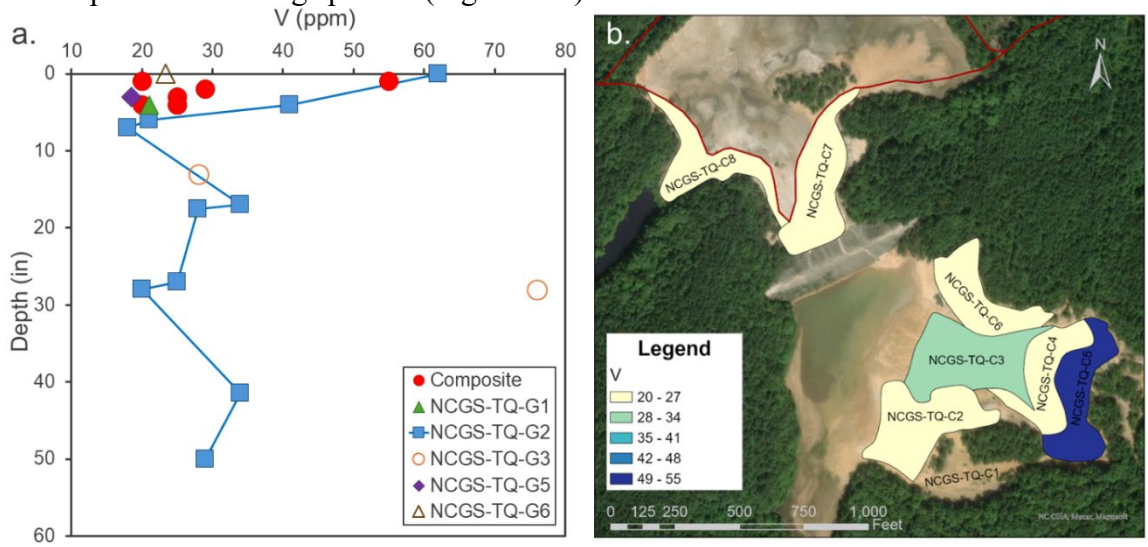

Figure 17. a. V concentration versus depth for composite and grab samples. b. Heat map for V concentration (ppm) in composite samples. Darkest blue represents the highest values with yellow representing the lowest. See text for more information.

Grab sample V concentrations range from 18 to 76 ppm, with mean of 32 ppm and a median value of 28 ppm. The highest concentrations are in NCGS-TQ-G3-28-30 (76 ppm) and NCGS-TQ-G2-0-4 (62 ppm; Figure 17a).

Drill core samples have V concentrations from 12 to 28 ppm, with a mean of 22 ppm and a median of 23 ppm. The highest concentration is in NCGS-TQ-D1-23-24. None of the cores exhibit spikes of notably high concentrations, however in general, cores 1 and 7 in tailings pond 3 have higher V content than the cores in tailings pond 2 (Figure 18).

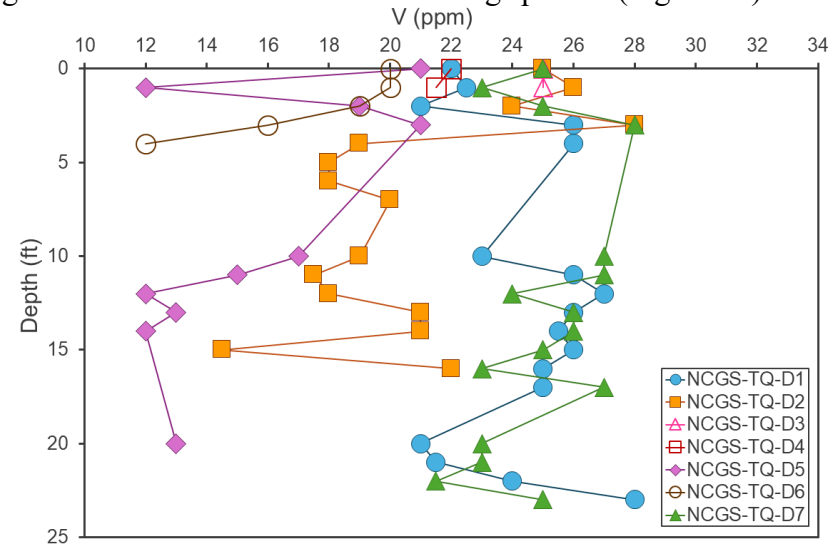

Figure 18. V concentration versus depth for Tungsten Queen Cores. See text for more information.

Beryllium

Composite sample Be concentrations range from 7 to 12 ppm (Figure 19a), with the highest concentration in sample NCGS-TQ-C8, located in the southeastern portion of tailings pond 3 (Figure 19b). The mean and median Be concentration for composite samples is 8 ppm.

Grab sample Be concentrations range from 6 to 21 ppm (Figure 19a) with a mean of 11 ppm and a median of 9 ppm. The highest grab sample Be concentrations are from NCGS-TQ-G3-28-30 (21 ppm), NCGS-TQ-G1 (17 ppm), and NCGS-TQ-G2-41.5-50 (17 ppm; Figure 19a).

Four sonic core samples have Be concentrations below detection limit (<5 ppm; NCGS-TQ-D5-0-1, NCGS-TQ-D5-12-13, NCGS-TQ-D5-20-21, NCGS-TQ-D6-4-4.7), while the rest range from 6 to 19 ppm, with a mean of 11 ppm and a median of 10 ppm. The highest core sample concentrations are NCGS-TQ-D3-1-2 (19 ppm) and NCGS-TQ-D7-12-13 (18 ppm; Figure 20).

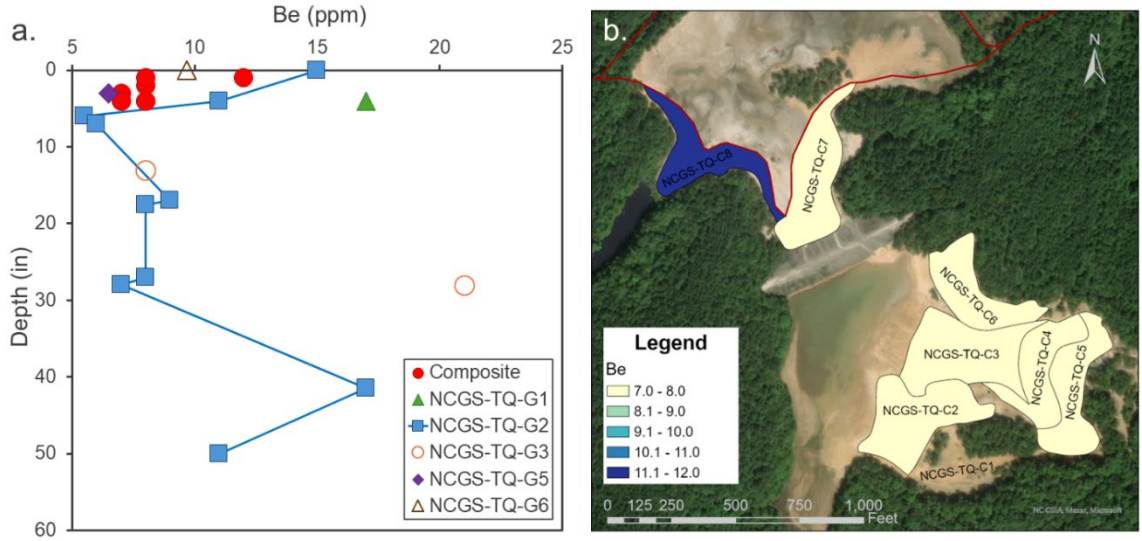

Figure 19. a. Be concentration versus depth for composite and grab samples. b. Heat map for Be concentration (ppm) in composite samples. Darkest blue represents the highest values with yellow representing the lowest. See text for more information.

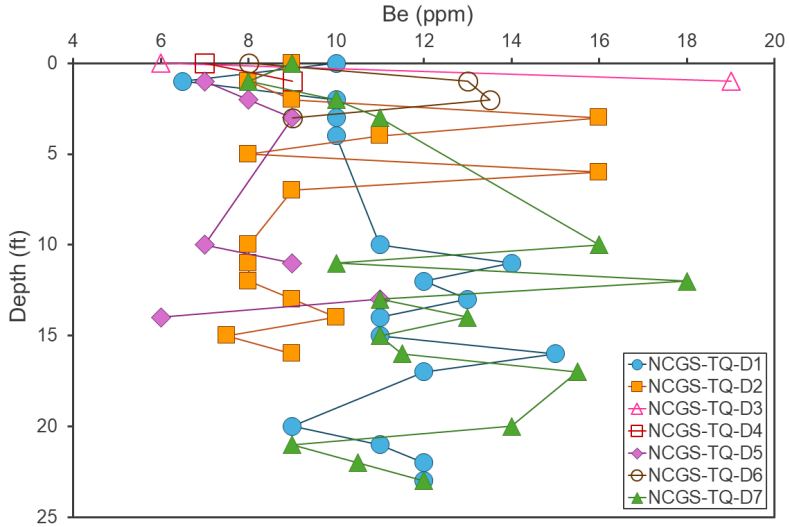

Figure 20. Be concentration versus depth for Tungsten Queen Cores. See text for more information.

Bismuth

Composite sample Bi concentrations range from 7.4 to 24.7 ppm (Figure 21a), with the highest concentrations in NCGS-TQ-C5, located in the eastern portion of tailings pond 2 (Figure 21b). The mean concentration is 12 ppm while the median is 11 ppm.

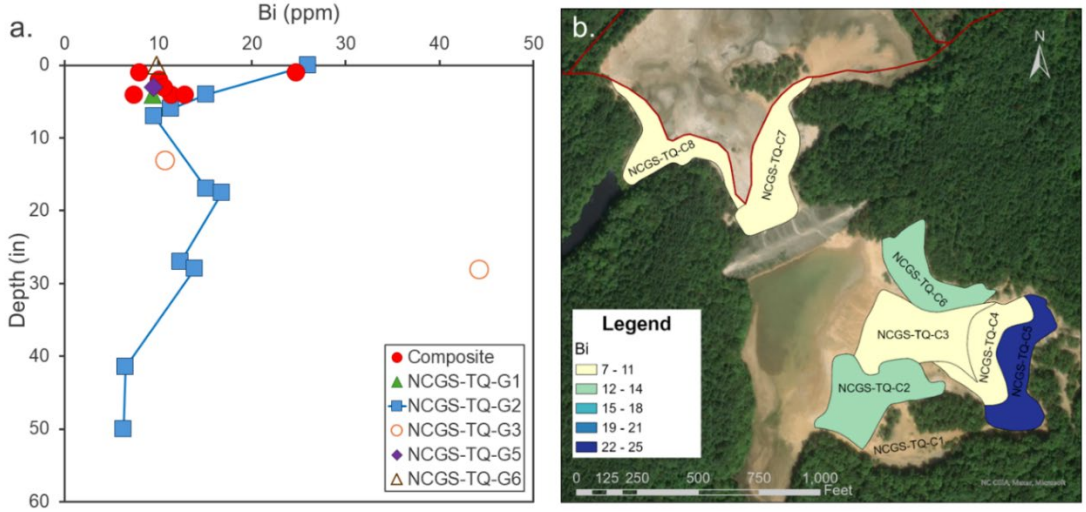

Figure 21. a. Bi concentration versus depth for composite and grab samples. b. Heat map for Bi concentration (ppm) in composite samples. Darkest blue represents the highest values with yellow representing the lowest. See text for more information.

Grab sample Bi concentrations range from 6.3 to 44.2 ppm, though most samples fall within the same range as the composite samples (Figure 21a). The grab samples have a mean Bi concentration of 14 ppm and a median of 11 ppm. The highest grab sample Bi concentrations are from NCGS-TQ-G3-28-30 (44.2 ppm) and NCGS-TQ-G2-0-4 (26 ppm; Figure 21a).

Drill core samples range from 3.3 to 20 ppm Bi, with a mean of 9 ppm and a median of 8 ppm. The highest concentrations are NCGS-TQ-D6-3-4 (20.0 ppm) and NCGS-TQ-D5-11-12 (19.0 pm), however, NCGS-TQ-D6-0-1, NCGS-TQ-D6-1-2, and NCGS-TQ-D6-4-4.7 also have similarly elevated Bi (18.0 ppm, each), as do NCGS-TQ-D7-2-3 (17.5 ppm) and the NCGS-TQ-D5-3-4.4 (17.0 ppm; Figure 22).

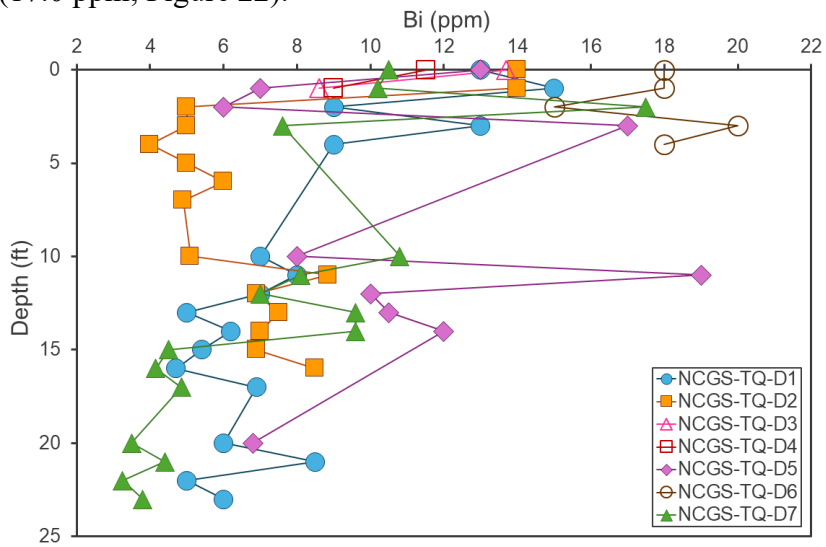

Figure 22. Bi concentration versus depth for Tungsten Queen Cores. See text for more information.

Gallium

Composite sample Ga concentrations range from 3 to 8 ppm, although six of the seven samples contain ≤ 4 ppm (Figure 23a). The mean Ga content of composite samples is 4 ppm while the median is 3 ppm. The highest concentration is in NCGS-TQ-C5, located in the eastern portion of tailings pond 2 (Figure 23b).

Grab samples have 3 to 23 ppm Ga (Figure 23a), with a mean of 8 ppm and a median of 6 ppm. The highest concentrations are from NCGS-TQ-G3-28-30 (23 ppm) and NCGS-TQ-G2-0-4 (17 ppm).

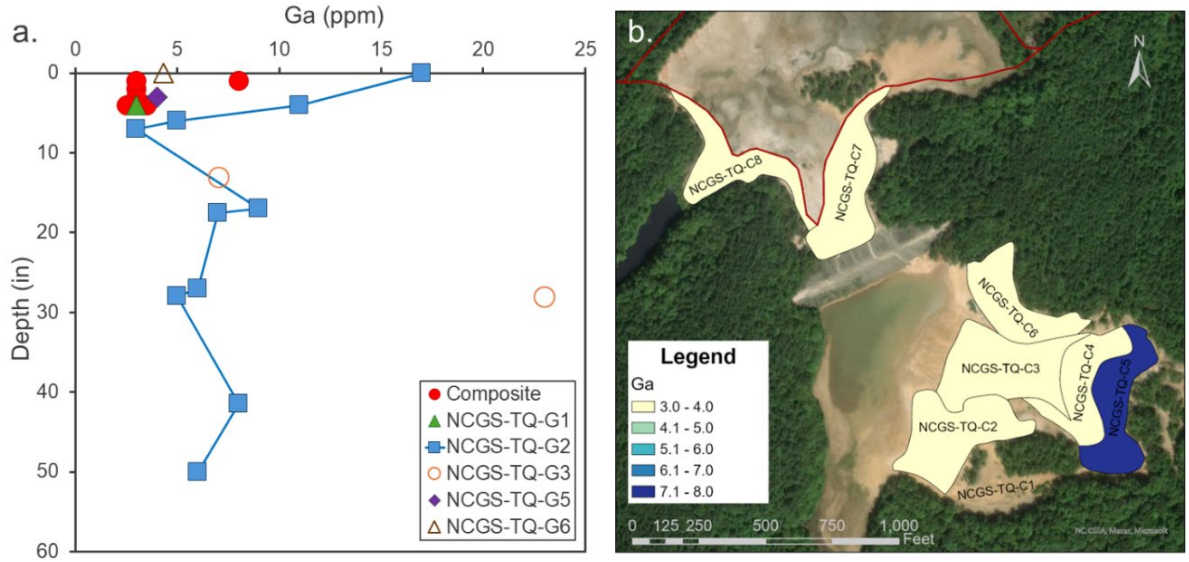

Figure 23. a. Ga concentration versus depth for composite and grab samples. b. Heat map for Ga concentration (ppm) in composite samples. Darkest blue represents the highest values with yellow representing the lowest. See text for more information.

Drill core samples contain Ga concentrations from 2 to 6 ppm, with a mean and median of 5 ppm. None of the cores exhibit notably enriched intervals (Figure 24).

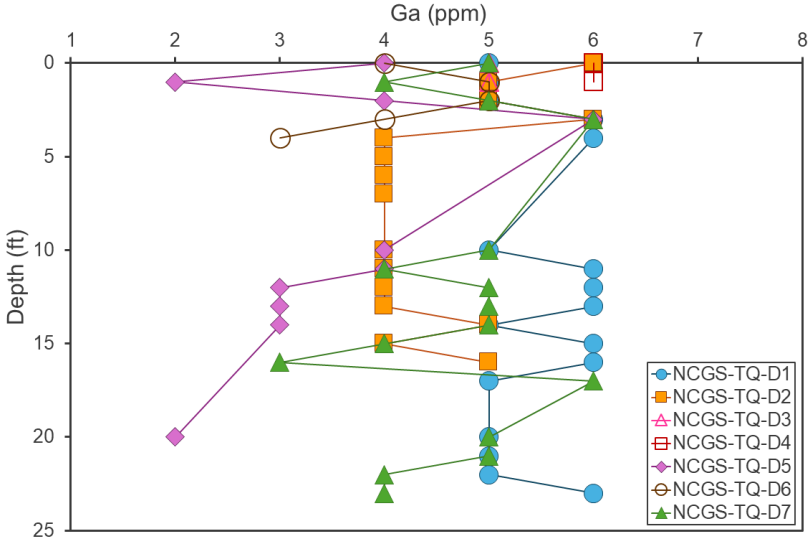

Figure 24. Ga concentration versus depth for Tungsten Queen Cores. See text for more information.

Germanium

All composite samples contain 2 ppm Ge (Figures 25a and 25b) while all grab samples have 2 or 3 ppm (Figure 25a) with a mean and median grab sample concentration of 2 ppm. Core samples range from 2 to 5 ppm Ge, with the highest values (5 ppm) in NCGS-TQ-D5-20-21, NCGS-TQ-D7-0-1, NCGS-TQ-D7-1-2, NCGS-TQ-D7-16-17, and NCGS-TQ-D7-17-18.4 (Figure 26). The mean and median concentration of Ge in cores is 3 ppm.

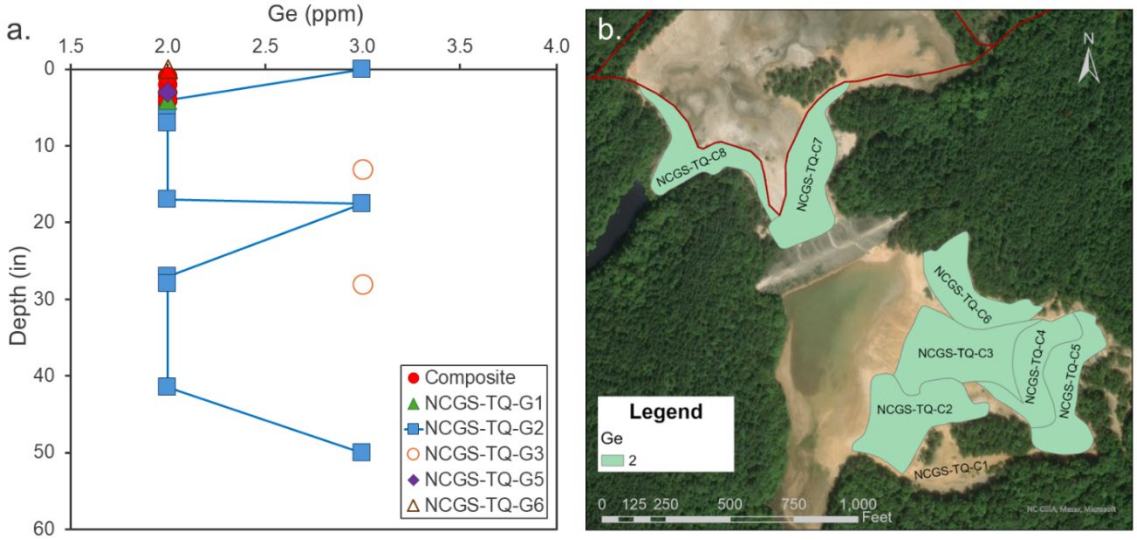

Figure 25. a. Ge concentration versus depth for composite and grab samples. b. Heat map for Ge concentration (ppm) in composite samples. Darkest blue represents the highest values with yellow representing the lowest. See text for more information.

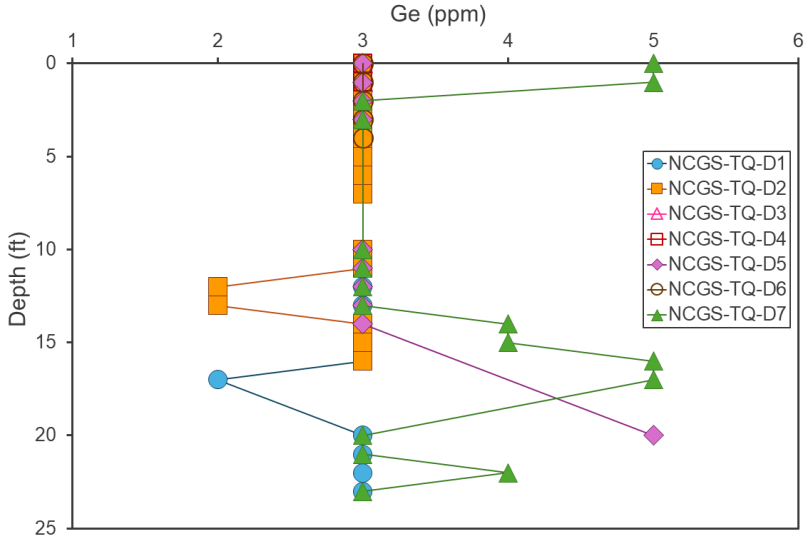

Figure 26. Ge concentration versus depth for Tungsten Queen Cores. See text for more information.

4.2 Potential Non-Critical Mineral Commodities

Silver

Composite sample Ag concentrations range from 9 to 21 ppm (Figure 27a), with the highest concentration in NCGS-TQ-C5, located in the eastern portion of tailings pond 2 (Figure 27b). The mean and median Ag content of composite samples is 15 ppm.

Grab sample Ag concentrations range from 11 to 32 ppm, with a mean of 17 ppm and a median of 15 ppm. The highest concentration is in NCGS-TQ-G3-28-30 (32 ppm; Figure 27a),

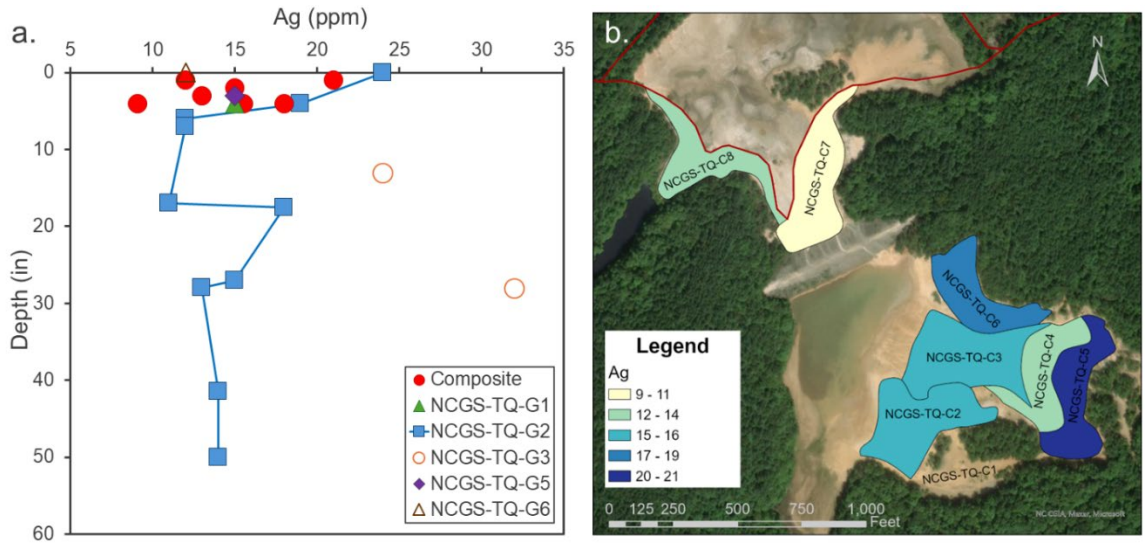

Figure 27. a. Ag concentration versus depth for composite and grab samples. b. Heat map for Ag concentration (ppm) in composite samples. Darkest blue represents the highest values with yellow representing the lowest. See text for more information.

while samples NCGS-TQ-G2-0-4 and NCGS-TQ-G3-13-17 also have elevated Ag (24 ppm each).

Drill core Ag concentrations range from 6.97 to 42 ppm, with a mean of 14 ppm and a median of 12 ppm. The highest Ag concentrations are in NCGS-TQ-D6-3-4 (42 ppm) and NCGS-TQ-D6-4-4.7 (Figure 28).

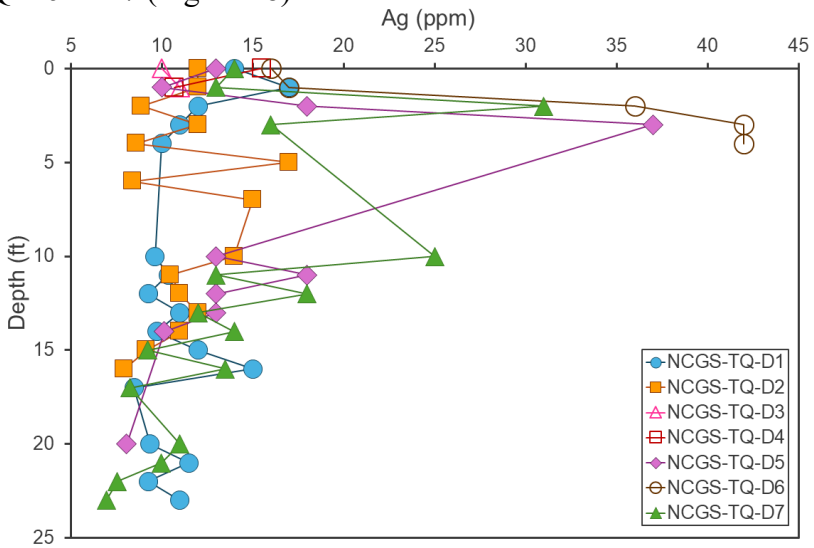

Figure 28. Ag concentration versus depth for Tungsten Queen Cores. See text for more information.

Gold

Composite sample Au concentrations range from 7 to 45 parts per billion (ppb; Figure 29a), with the highest concentration in NCGS-TQ-C5, located in the eastern portion of tailings pond 2 (Figure 29b). The mean and median for composite samples are both 22 ppb.

Grab sample Au concentrations range from 8 to 49 ppb (Figure 29a) with a mean of 19 ppb and a median of 14 ppb. The highest Au concentrations are in samples NCGS-TQ-G1 (49 ppb) and NCGS-TQ-G2-50-53 (36 ppb).

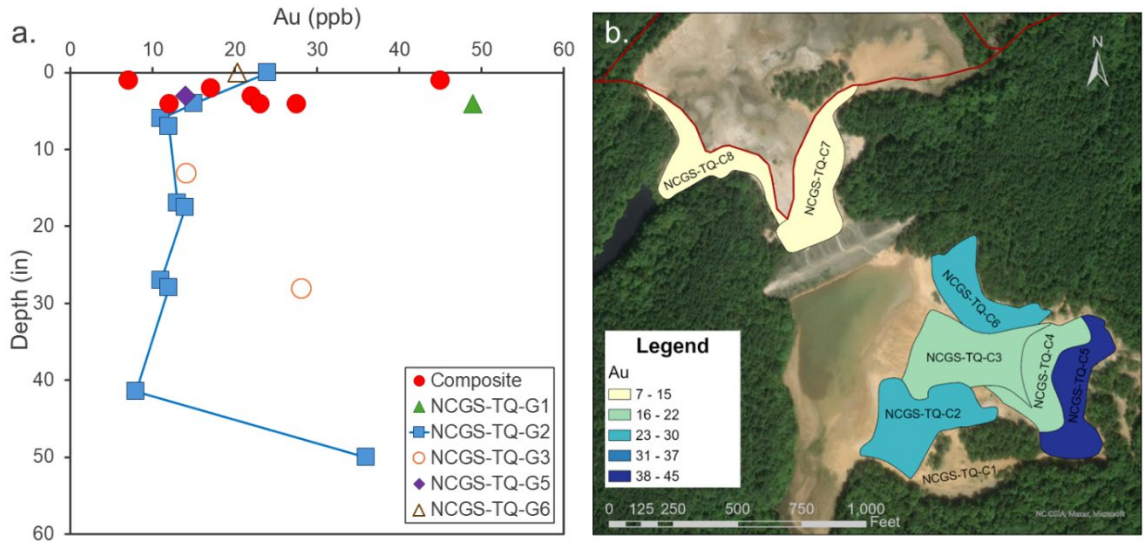

Figure 29. a. Au concentration versus depth for composite and grab samples. b. Heat map for Au concentration (ppb) in composite samples. Darkest blue represents the highest values with yellow representing the lowest.

Drill core Au concentrations range from 6 to 132 ppb, with a mean concentration of 39 ppb and a median of 36 ppb. The highest Au concentrations are in NCGS-TQ-D6-4-4.7 (132 ppb) and NCGS-TQ-D5-3-4.4 (129 ppb; Figure 30).

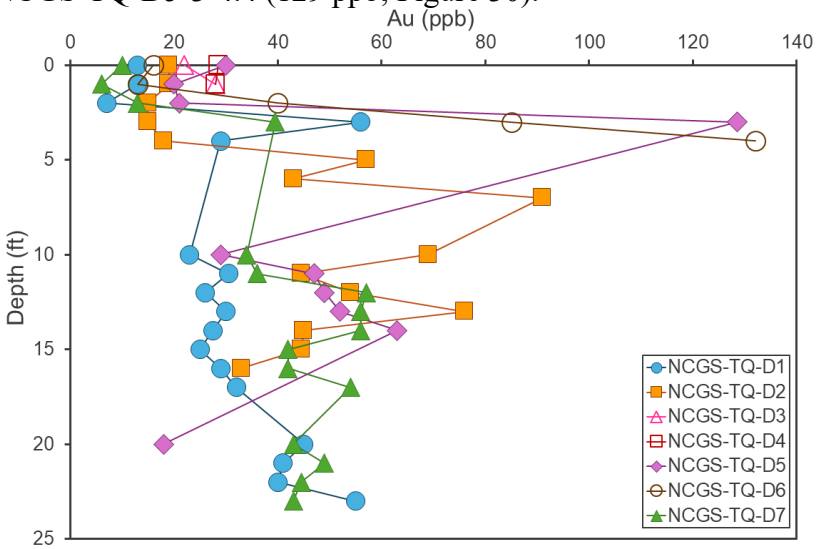

Figure 30. Au concentration versus depth for Tungsten Queen Cores. See text for more information.

5. Discussion

5.1 Potential Factors Controlling Critical Mineral and Non-Critical Commodity Distribution within Ponds

Several samples have the highest concentrations for their sample type in one or two elements, however, a handful of samples emerged as being especially concentrated in multiple elements (Table 3). Sample NCGS-TQ-G3-28-30 contains concentrations of W, F, Bi, Zn, Be, As, Sb, Te, V, Ga, and Ag elevated above other samples in this study, while sample NCGS-TQ-G2-0-4 has elevated W, F, Bi, As, Te, V, and Ga. Both samples were collected from profile intervals dominantly composed of clay to silt with very fine sand (Appendix 3). The elevated W content of the two samples aligns with the findings of Meyertons (1975), who report a positive relationship between sample W concentration and slime content as determined using a 400 mesh

sieve. Although clay and silt-dominated tailings samples are rare in this study's data set, these results could suggest that other critical minerals may be concentrated in fine size fractions as well.

Table 3. Samples Notably Enriched in the Most Elements

Sample Number	Enriched Elements
NCGS-TQ-C5	Mn, Bi, As, Sb, Te, V, Ga, Ag, Au
NCGS-TQ-G2-0-4	W, F, Bi, As, Te, V, Ga
NCGS-TQ-G3-28-30	W, F, Bi, Zn, Be, As, Sb, Te, V, Ga, Ag
NCGS-TQ-D5-3-4.4	W, Mn, As, Sb, Te, Au
NCGS-TQ-D6-3-4	W, Bi, As, Sb, Te, Ag

Sample NCGS-TQ-C5 is elevated in Mn, Bi, As, Sb, Te, V, Ga, Ag, and Au content when compared to other composite samples, while NCGS-TQ-D5-3-4.4 (W, Mn, As, Sb, Te, and Au) and NCGS-TQ-D6-3-4 (W, Bi, As, Sb, Te, and Ag) are enriched in more critical minerals and non-critical commodities than other core samples. Most of the critical minerals enriched in these three samples were also elevated in the clay-to-silt-dominated NCGS-TQ-G3-28-30 and/or NCGS-TQ-G2-0-4. However, NCGS-TQ-C5 is composed primarily of very fine to very coarse sand with <5% mud (Appendix 3), making the sample's grainsize unremarkable in this dataset. Visual analysis indicates NCGS-TQ-D5-3-4.4 and NCGS-TQ-D6-3-4 are also sand-dominated, skewing toward very fine to fine sand grainsizes with an estimated 10 to 15% mud (Appendix 3). The mud content of NCGS-TQ-C5, NCGS-TQ-D5-3-4.4, and NCGS-TQ-D6-3-4 fall within the range of samples that are not notably critical minerals-enriched, suggesting clay and silt content may not cause the elevated concentrations of multiple critical minerals in these three samples. However, NCGS-TQ-C5 represents the portion of tailings pond 2 directly below the gravity separator location, while cores 5 and 6 are the closest cores to the gravity separator (Figure 2). These data could suggest proximity to the gravity separator is an important control on critical mineral content in some samples.

Many of the critical and non-critical commodities concentrated in certain samples near the gravity separator are found in minerals with a density ≥5g/cm^3, such as hubnerite (W), pyrite (As), tetrahedrite (Sb), altaite (Te), wittichenite (Bi), volynskite (Ag), and Au. The higher density could concentrate these minerals closer to their point of entry, contributing to lateral variations in tailings impoundment critical mineral distribution. However, any generalized relationship between mineral density and gravity separator proximity may primarily apply to sand-rich samples. Meyertons (1975) noted high W in the slime-rich zone 4 of his report, which is located in the northeastern portion of tailings pond 3 far from the gravity separator. It is possible the finer grainsize may partially compensate for the higher density allowing the particles to move further from their point of origin.

Vertical variability also exists in the Tailings Pond 2, as exhibited by the differences in critical mineral and non-critical commodity content of samples from cores 5 and 6. Density differences could contribute through a downward migration of denser minerals, especially in finer size fractions. However, the observed depth-related variations may primarily result from heterogeneities in the ore being processed at a given time. For example, the similar depths of enriched samples in cores 5 and 6 could suggest a particularly critical mineral-rich flux of tailings that extended to core 5 but not as far as core 2.

Data from this study and Meyertons (1975) suggest density and grainsize variations may produce lateral variability in critical mineral content of the tailings impoundment, while deposit heterogeneity may cause vertical variations. Collectively, these observations could have interesting implications for the relationship between grain size, mineral density, vein heterogeneity, and the distribution of critical mineral and non-critical commodity concentrations in the tailings ponds.

5.2 Variations Between Ponds

Bivariate geochemical plots suggest potentially interesting differences between ponds 2 and 3 that could reflect compositional variability in hubnerite and possibly some sulfides. When W concentrations are plotted versus Mn concentrations (Figure 31), samples from tailings ponds 2 and 3 seem to follow two separate trends. Thus, for a given Mn concentration, samples from tailings pond 3 tend to have lower W than samples from tailings pond 2. These different trends likely result from natural variability in the composition of hubnerite combined with how tailings were dispersed through the pond during mining operations.

A few samples fall noticeably off the trends for Mn vs W in Figure 31. NCGS-TQ-G1 and NCGS-TQ-G5 (purple box in Figure 31) have abundant dark minerals which give them a "salt and pepper" look. These samples plot among the highest for Mn, but do not have elevated W concentrations, suggesting hubnerite is not responsible for their high Mn. Another "salt and pepper" sample, NCGS-TQ-G3-13-17 (yellow box in Figure 31) also falls off the overall tailings pond 3 trend, but to a lesser extent than NCGS-TQ-G1 and NCGS-TQ-G5. Rhodochrosite and ankerite, both reported to comprise <0.1% of the deposit (Casadevall and Rye, 1980), could be sources of Mn in these samples. Espenshade (1945) also notes the presence of a golden-brown garnet in the deposit, and the authors cite C.S. Ross as concluding it is probably "spessartite", interpreted here to be spessartine based on the presence of garnet noted in other sources (e.g., Foose et al., 1980). If spessartine garnet is present in the tailings pond, it could also contribute Mn without elevating the W content of the samples. The presence of Mn-rich, W-poor mineral(s) may contribute to scatter in the Figure 31 data beyond the outlier "salt and pepper" samples.

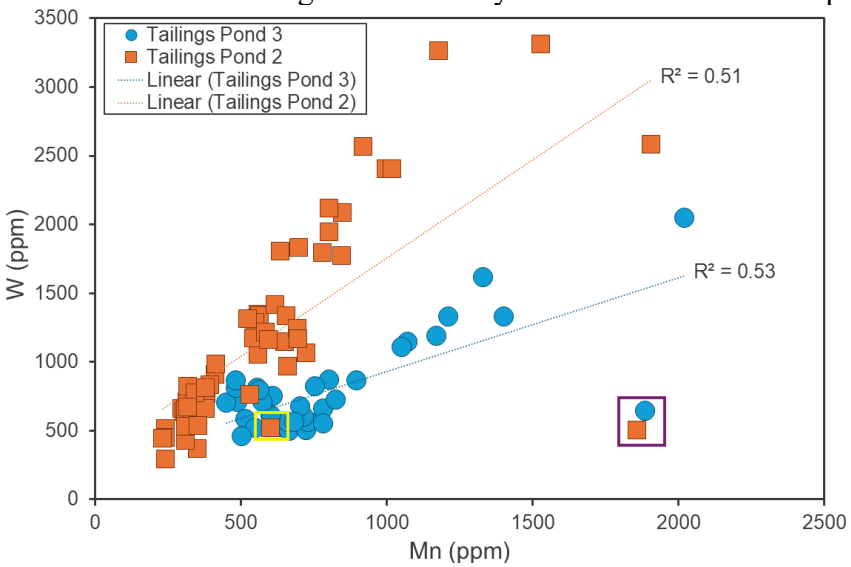

Figure 31. a. Plot of Mn concentration versus W concentration for all samples, coded according to tailings pond. Purple box highlights NCGS-TQ-G1 and NCGS-TQ-G5, the "salt and pepper" samples with very high Mn but lower W. Yellow box highlights NCGS-TQ-G3-13-17, which is also a salt and pepper sample that falls off the tailings pond 2 trend, but shows less Mn-enrichment relative to W. See text for more information.

However, more advanced mineralogical analysis is needed to confidently identify them and constrain their abundance.

The critical minerals Sb, As, and Te also show some variability between ponds when plotted versus sulfur (S) concentration (Figures 32-34). In all three plots, tailings pond 3 data show some degree of a trend between the critical mineral and S, while tailings pond 2 data show more scatter at low S concentrations with an additional three data points with high S values. These three points, NCGS-TQ-D6-3-4, NCGS-TQ-D6-4-4.7, and NCGS-TQ-D5-3-4.4, are located near the gravity separator which may contribute to an enrichment in sulfide minerals. Tailings pond 3 samples have a more continuous range of S concentrations and, for a given S content, tend to have lower Sb, As, and Te concentrations than tailings pond 2 samples, at least for S <~4,000 ppm (Figures 32-34). Variability in the critical mineral concentrations in sulfide minerals, and/or differing abundance of various sulfide minerals between the ponds could be a factor in the observed inter-pond variations.

In addition to natural variability in mineral compositions, enhanced weathering could also influence the compositional differences between ponds. The mining and processing of ore and disposal of waste as tailings introduces oxygen, which promotes sulfide mineral oxidation and can result in acid rock drainage and metal leaching (International Network for Acid Prevention, 2009). Thus, different conditions related to mineralogy, microbiome, pH, tailings permeability, etc., could produce variability in sulfide mineral breakdown and by extension metal leaching between ponds. These conditions could especially impact critical minerals held in sulfide minerals, which might account for the data scatter of Figure 31.

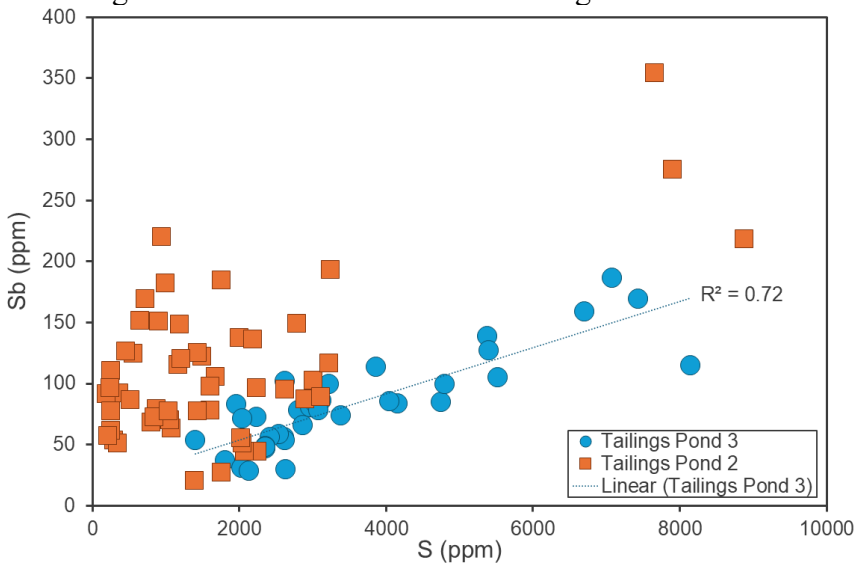

Figure 32. S concentration versus Sb concentration for all samples. See text for more information.

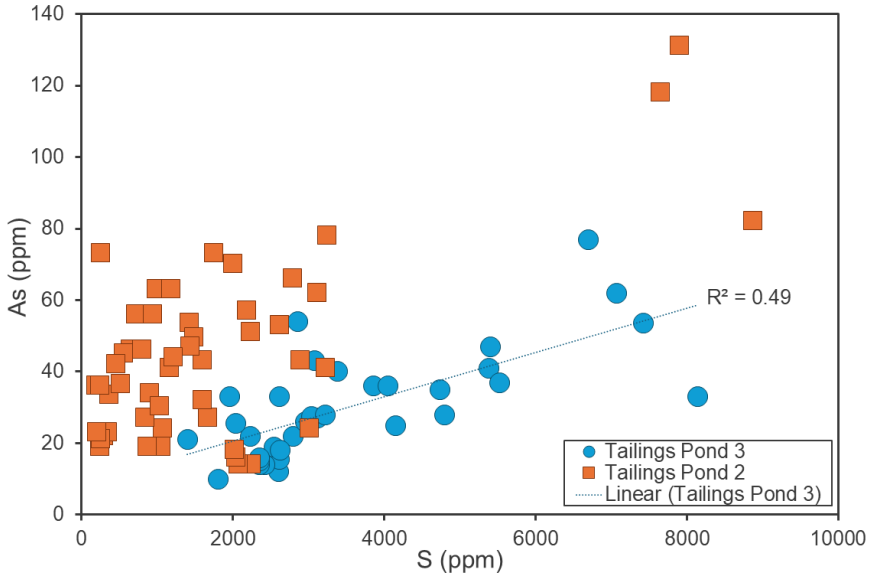

Figure 33. S concentration versus As concentration for all samples. See text for more information.

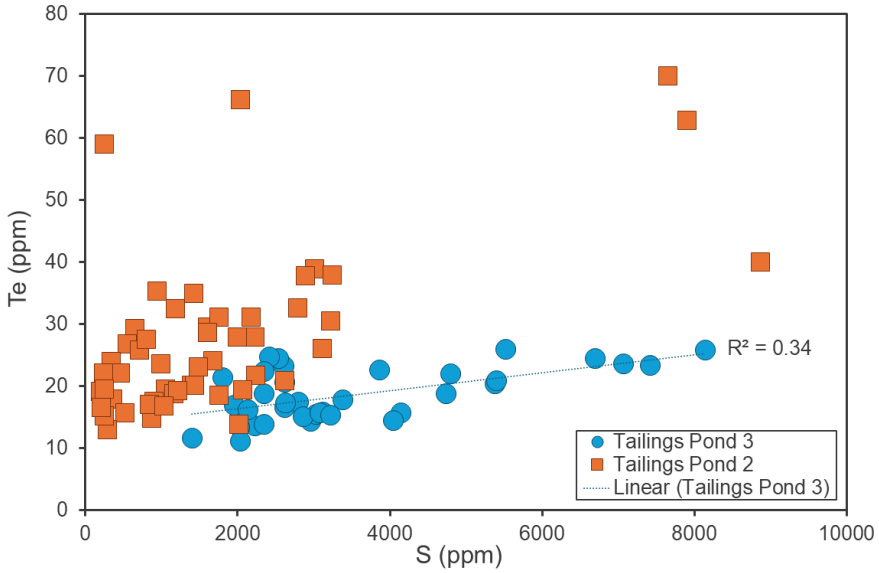

Figure 34. S concentration versus Te concentration for all samples. See text for more information.

5.3 Principal Component Analysis

Prior to principal component analysis (PCA), the dataset was assessed for elements to be included in PCA. In addition to the fourteen elements chosen as the main focus of this study (F, W, Mn, Sb, Be, Bi, Te, Zn, As, Ga, Ge, V, Au, and Ag), nine elements were added for PCA based on the Tungsten Queen deposit mineralogy and/or their presence on the 2022 USGS Critical Mineral List. Sulfur and Pb were included because of their presence in Tungsten Queen vein minerals (Table 1), while critical minerals lithium (Li), rubidium (Rb), yttrium (Y), cesium (Cs), dysprosium (Dy), erbium (Er), and ytterbium (Yb) were included because their concentrations are above the analysis detection limit. Thus, the following 23 elements were used for PCA: Li, Be, F, S, V, Mn, Zn, Ga, Ge, As, Rb, Y, Ag, Sb, Te, Cs, Dy, Er, Yb, W, Au, Pb, and Bi. Data were then transformed and normalized prior to PCA to make the dataset into one of independent variables not affected by the sum-constant or "closure" problem (Chayes, 1960; Le Maitre, 1982; Aitchison, 1984; Greenacre, 2021). Data were transformed using the centered log-

ratio transformation (Pawlowsky-Glahn et al., 2015), and data were then normalized using the median and standard deviation (Boschetty et al., 2022). The PCA was performed using the freeware program R (R Core Team, 2022).

PCA results are given in Figure 35 and in the "PCA Results" tab of Appendix 4, while eigenvectors used to draw the vectors in Figure 35 are provided in the "PCA Eigenvectors" tab of Appendix 4. Principal component 1 accounts for 37% of the variance in the dataset, and principal component 2 accounts for 23% of the variance. Grab samples are dominated by positive principal component 1, and composite samples are dominated by negative principal component 2. Drill core samples are dominated by negative principal component 2 but have the widest scatter on Figure 35. Eigenvectors of W and Mn both plot in quadrant 3 (negative

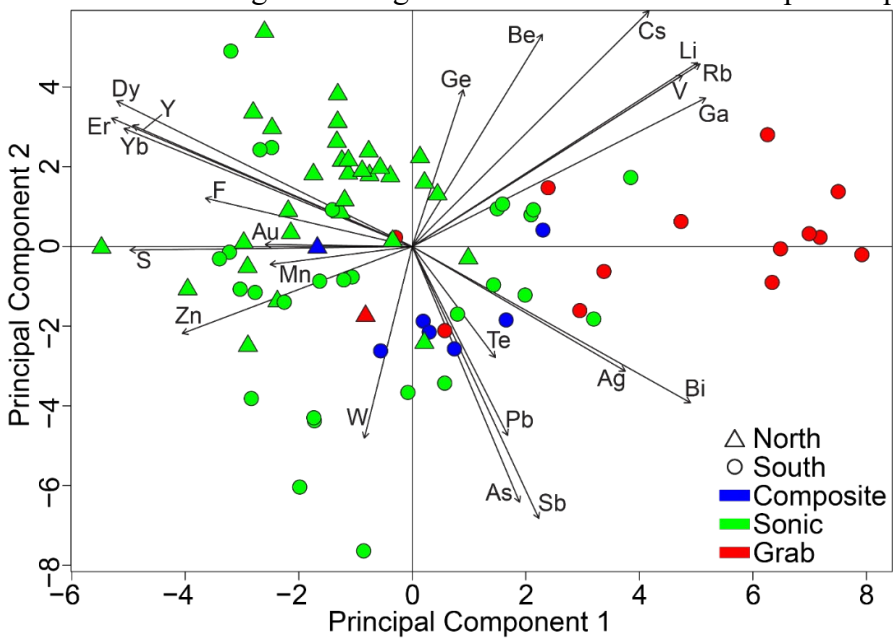

Figure 35. Results of PCA. Eigenvectors used to draw vectors are provided in Appendix 4.

principal components 1 and 2), with S and Zn. Other major elements related to sulfide minerals, Pb and As, plot in quadrant 4 (positive principal component 1, negative principal component 2), along with Te, Ag, Sb, and Bi. Quadrant 1 (positive principal components 1 and 2) contains Ga, Ge, Be, Cs, Li, Rb, and V, and quadrant 2 (positive principal component 2, negative principal component 1) contains F, Au, Y, Dy, Er, and Yb. The rare earth elements (REE) used in this PCA (Dy, Er, Yb, and Y) cluster together in PCA space, and Rb and V also closely align in PCA space (Figure 35).

The PCA results shown in Figure 35 are complementary to the bivariate plots in Section 5.2, and these PCA results can sometimes be correlated to mineral chemistry. For instance, hubnerite elements Mn and W are positively correlated in Figure 31, and their PCA eigenvectors point in the same quadrant in Figure 35, indicating that they behave similarly in this geochemical dataset. The sphalerite elements Zn and S also plot in the same quadrant, showing that the mineralogy of this particular sulfide is coherent in PCA. Other sulfide-related elements like Pb, Sb, As, and Te, plot together in quadrant 4, away from S. This could indicate a breakdown of certain sulfide minerals in the tailings impoundment over time. In addition, REE (Y, Dy, Er, and Yb) have eigenvectors in quadrant 2 of Figure 35, which is logical given their geochemical affinity. Further detailed mineral chemistry analysis would be needed to discern in which phases these REE are residing.

5.4 Volume Calculations

The bulk mine tailings analysis consisted of entering 1) contour lines from a pre-tailings topographic map; 2) an area of interest polygon; and 3) contour lines from a modern (2020) LiDAR-derived digital elevation model (DEM) into an Esri ArcGIS Pro, version 3.2 workflow. The first step in the workflow was necessary for determining a pre-tailings ground surface. Since large-scale mining began in mid-1943, topographic map contours from a 1943 mineral investigation summary report (White, 1943) were georeferenced as a starting point for the pre-tailings surface (Figure 36). To better constrain the actual pre-tailings surface and account for ground surface modifications not reflected in the topographic map, pre-tailings ground surfaces at NCGS-drilled core locations (NCGS-TQ-D1 through NCGS-TQ-D7; Figure 36) were constrained from the difference between the modern elevation at the core location and the depth to the bottom of the tailings in each core (surface elevation – depth to contact). Additionally, nine control points (CP-01 through CP-09; Figure 36) were added to the map and assigned elevations according to LiDAR data, in order to establish control in areas away from core locations where the tailings thicknesses are known to be shallow. This technique was available and necessary in the floodplain, the northern border of tailings pond 3 adjacent to Island Creek, and in a triangular pattern on the perimeter of a grove of trees. All control points are located in USACE-owned portions of the tailings ponds since access was not granted to that property.

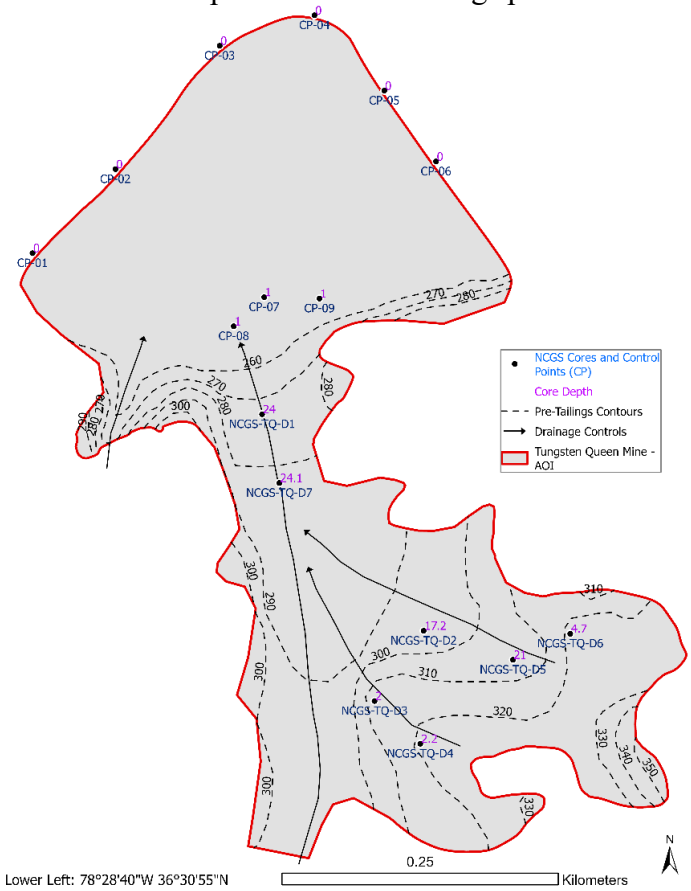

Figure 36. Pre-tailings raster surface with georeferenced 1943 topographic map contours, NCGS sonic core depths control points, and drainage controls. See text for details.

"Drainage Control" lines were added to the analysis features in order to force the surface down gradient in preparation for converting the pre-tailings features to a raster surface. Drainage

control lines were digitized based on expected hydrologic flow paths within the study area. These lines helped enforce topographic realism by ensuring the interpolated pre-tailings surface drained correctly toward known low points, particularly near Island Creek and floodplain margins. Their inclusion prevents the formation of artificial sinks or topographic anomalies during interpolation that could distort tailings thickness estimates.

The surface modeling assumes a relatively continuous and linear tailings fill between known points (e.g., cores and control points). In areas far from core locations or where the historic contours were tightly spaced and complex, the interpolation may oversimplify natural terrain variation. Additionally, drainage lines were assumed to follow natural flow paths unaffected by historic mining modifications, which may not reflect all anthropogenic alterations. These factors introduce some degree of uncertainty into the modeled pre-tailings surface, particularly in unmodeled or inaccessible parts of the study area (e.g., USACE land or beneath a dense stand of vegetation). Nevertheless, control point elevation matching and alignment with mapped drainage reduced the likelihood of significant bias.

The pre-tailings raster surface (Figure 36) was created with the "topo-to-raster" analysis tool available in Esri ArcGIS Pro. The tool's parameters were aligned in the following ways: (1) the drainage patterns were enforced as a way to remove all sinks or depressions; (2) the depth of the cores were used as the first order algorithm enforcement control; and (3) the vertical standard of error was set to 2 ft because the dataset has significant random (non-systematic) vertical errors with uniform variance, which stabilizes convergence when rasterizing point data with drainage control data.

After the pre-tailings surface raster was created, the "raster calculator" tool was used to determine the modern surface -to- pre-tailings surface thickness differential. A conditional statement was then applied to eliminate all derived thickness patterns with a negative value. This outcome was minimal, and in all cases, the negative value was close to zero. This effect occurred either because the model algorithm had difficulty negotiating tight contour intervals far from a core control point or because there actually was less fill (a possibility near the tailings perimeter).

The mine operators constructed a dam in 1970, neatly segmenting the area of interest (tailings impoundment) close to the north-to-south halfway line. This dam was constructed to impound additional tailings from the brief resurgence in operations before the mine's final closure in 1971 (Meyertons, 1975). The dam's dimensions were estimated from aerial imagery and approximated to 20 ft in height, 20 ft in width, and 500 ft in length. The 200,000 ft^3 determined from these dimensions was eventually subtracted from the total bulk volume.

Finally, the "surface volume" tool in Esri ArcGIS Pro was used to calculate the area and volume of mine tailings (above a plane height of zero). After subtracting the estimated volume of the causeway, the estimated volume of the mine tailings was determined to approximate 43,400,000 ft^3 (Figure 37). The symbology used to segment the tailings' thickness was a 1/2 standard deviation interval size scheme.

Meyertons (1975) reported a total tailings volume of 42,100,000 ft^3, however, this estimate includes their "zone 1," which they describe as coarse sand at the base of the Tungsten Mining Corporation mill. NCGS staff were unable to find tailings in the vicinity of the old mill, suggesting they may have been removed as part of the environmental remediation effort at the site. To facilitate a more accurate comparison, the volume Meyertons (1975) calculated for zone 1 tailings was removed from his total estimate, leaving 40,500,000 ft^3 as the volume of tailings in the tailings impoundment. Thus, this study's estimate of 43,400,000 ft^3 represents a net 6.7% increase over the estimate of Meyertons (1975).

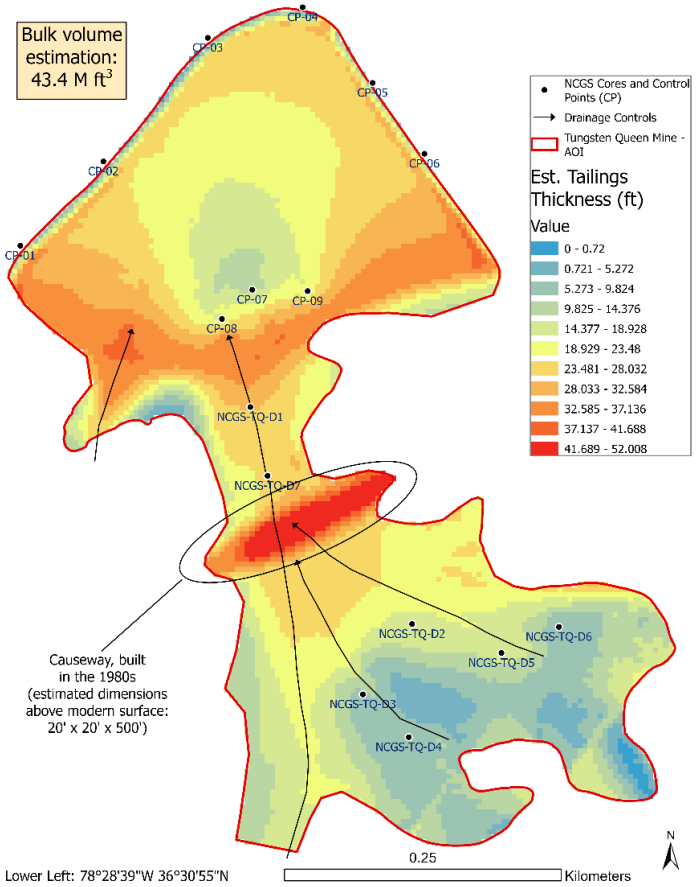

Figure 37. Tungsten Queen mine tailings isopach and bulk volume estimate. See text for details.

This study's analysis evaluated the volume of tailings in ponds 2 and 3 since the tailings from pond 1 had been previously removed, as confirmed by the abundance of regolith observed during sampling and the geochemical composition of composite sample 1. It has been reported that some tailings were pumped into the underground shafts during operations to raise the floor of the mine so additional areas of the vein could be accessed. However, the present study is not able to include those tailings in the volume or resource estimates due to a lack of relevant records.

5.5 Critical Mineral Resource Estimates

The total mass of the tailings was calculated using Equation 1:

$$\textit{Total mass of tailings} = \textit{volume of tailings} \times \textit{density of tailings} \quad \text{(eq. 1)},$$

where the total volume of the tailings (calculated above) was 43,400,000 ft^3 and 125 lb/ft^3 (which corresponds to ~2.0 g/cm^3) was selected as a reasonable bulk density for the tailings. This yields a total mass of 5,425,000,000 lb or ~2,460,551,000 kg.

Tungsten Queen cores best represent the lateral and vertical compositional variability of the impoundment and thus were used to calculate weighted mean concentrations of critical minerals and non-critical commodities covered in this report (Table 4). Each core sample's concentration for a given element was weighted according to the length of the sample interval, which ranged from 0.7 to 1.4 ft. For four samples, As and V concentrations were below the

detection limit and assigned a concentration of zero for the weighted mean calculations. Additionally, F was converted from wt% to ppm and Au was converted from ppb to ppm.

Resource estimates for each commodity were calculated using Equation 2:

*Resource estimate = weighted mean concentration/1,000,000 * total mass of tailings* (eq. 2),

where the total mass of tailings is given in kg and the analyte weighted mean is in ppm. The resulting resource estimate in kilograms was divided by 1000 to convert to metric tons (t). Table 4 shows resource estimates in kg and t for all critical minerals and non-critical commodities discussed in this report. These resource estimates range from 66,695 t for F to 8 t for Ge.

This study's calculation suggests that 2,706 t W is contained in the Tungsten Queen tailings pond. Meyertons (1975) estimated 404,242 t WO_3 (320,552 t W) for all tailings, which equates to 386,851 t WO_3 (306,762 t W) without zone 1. This study's estimate is ~99% lower than Meyertons (1975) despite a larger estimated tailings volume. This could be due to many factors, including (a) the lower weighted mean WO_3 calculated by this study, which was 0.139 wt% versus 0.218 wt% for Meyertons (1975) or (b) this study's sampling limitations since the highest wt% WO_3 values reported by Meyertons (1975) were in a section of tailings pond 3 this study did not have permission to access. However, it is hard to reconcile two orders of magnitude difference between these estimates based on those factors. Given the input data of Meyertons (1975) used to calculate the resource estimate of WO_3 (including 0.218 wt% WO_3 and 2,038,000 "tons" of tailings) it seems possible that a decimal place error was involved during conversion and/or calculation of STU of WO_3 in that report.

Table 4. Weighted Mean Concentrations and Resource Estimates for Tungsten Queen Tailings

Critical Mineral	Weighted mean (ppm)	Resource Estimate (kg)	Resource Estimate (metric ton)
F	27,106	66,695,404	66,695
W	1,100	2,706,355	2,706
WO_3	1,387	3,412,931	3,413
Mn	704	1,732,457	1,732
Zn	600	1,476,222	1,476
Sb	100	245,367	245
As	37	92,183	92
Te	24	60,111	60
V	21.9	53,832	54
Be	10	24,622	25
Bi	9.0	22,108	22
Ga	5	11,430	11
Ge	3	7,720	8
Non-Critical Commodity	**Weighted Mean (ppm)**	**Resource Estimate (kg)**	**Resource Estimate (metric ton)**
Ag	14	34,349	34
Au	0.040	97	0.1

5.6 Acid-Base Accounting

The Tungsten Queen mine is listed as an NC Department of Environmental Quality Inactive Hazardous Site (ID# NCD082362989) with known soil and water contamination. The mine site is located approximately 2 miles southwest of the Island Creek Reservoir. The Island Creek Dam, which separates the Island Creek Reservoir from the larger John H. Kerr Reservoir, was constructed in 1955 to prevent flooding of the Tungsten Queen mine site and contains pump stations that move water from the Island Creek Drainage Basin into Kerr Reservoir. The United States Army Corps of Engineers (USACE) have expressed concern that Pb and other metals from the Tungsten Queen mine tailings could contaminate the Island Creek Reservoir (U.S. Army Corps of Engineers, 2017). This, in turn, would lead to contamination of the John H. Kerr Reservoir, which serves as a drinking water source for local municipalities. The leaching of metals by acid rock drainage is well established (e.g., International Network for Acid Prevention, 2009), and could cause the kind of metal contamination the U.S. Army Corps of Engineers (2017) expressed concern about. Thus, acid-base accounting (ABA) data were collected for all Tungsten Queen tailings samples to provide a cursory evaluation of the potential for net acid production by the tailings (Appendix 3).

ABA uses independent evaluations of the acid generating and acid neutralizing components to determine the net acid potential of the tailings (International Network for Acid Prevention, 2009). Two components, acid generation potential (AP) and neutralization potential (NP), are derived through these independent evaluations and are central to interpretations of ABA data. AP is determined using sulfur species in the samples, and S and AP have the theoretical relationship of: AP (kg CaC03/t) = 31.25 x S (%) (International Network for Acid Prevention, 2009). NP is determined from neutralizing compounds such as carbonates and exchangeable bases (Skousen et al., 2001). The NP and AP values are then used to calculate net neutralization potential (NNP) and neutralization potential ratio (NPR) through the following equations:

$$NNP = NP - AP \quad \text{(eq. 3)}$$

and

$$NPR = NP/AP \quad \text{(eq. 4)}.$$

NNP reflects the differences between a sample's potential to neutralize and form acid. Conceptually, a negative value would suggest a sample is acid producing, while a positive value is non-acid producing (Skousen et al., 2001). However, interpretations are trickier in practice, especially for NNP between -20 and 20 $kgCaCO_3/t$ (U.S. Environmental Protection Agency, 1994). While there has been significant disagreement on which NNP values indicate acid production and which do not (c.f., Skousen et al., 2001 and references therein), NNP >20 $kgCaCO_3/t$ is generally considered to be non-acid producing and NNP < -20 $kgCaCO_3/t$ is generally considered to be acid producing, while there is uncertainty for values between -20 and 20 $kgCaCO_3/t$ that may require kinetic testing (Fey, 2004).

NPR reflects the relative magnitude of NP and AP. It is more straight forward to interpret than NNP, however, interpretations are influenced by the two calcite neutralization reactions that can occur:

$$CaCO_3 + 2H^+ \rightarrow Ca^{2+} + H_2CO_3 \quad \text{(eq. 5)}$$

and

$CaCO_3 + H^+ \rightarrow Ca^{2+} + HCO_3^-$ (eq. 6).

Equation 5, which predominates at pH <6.3, requires half as much NP to neutralize one mole of H^+ as Equation 6, which primarily occurs at higher pH. This means a sample with an NPR < 1 will produce acid when conditions favor Equation 5, whereas an NPR >2 will be necessary to prevent acid production if conditions favor Equation 6. When pH is near neutral, both reactions can occur. Thus, NPR data are interpreted as potentially net acid generating for NPR < 1, not potentially net acid generating for NPR > 2, and uncertain if NPR is between 1 and 2.

NNP and NPR values for Tungsten Queen samples are shown in Figure 38, with most samples falling within the range of uncertainty for one or both parameters, suggesting kinetic testing may be necessary to more accurately evaluate the potential for net acid production. However, NCGS-TQ-D6-3-4 and NCGS-TQ-D6-4-4.7 plot in the net acid producing region for both NNP and NPR and are thus interpreted to be net acid producing. These two samples are

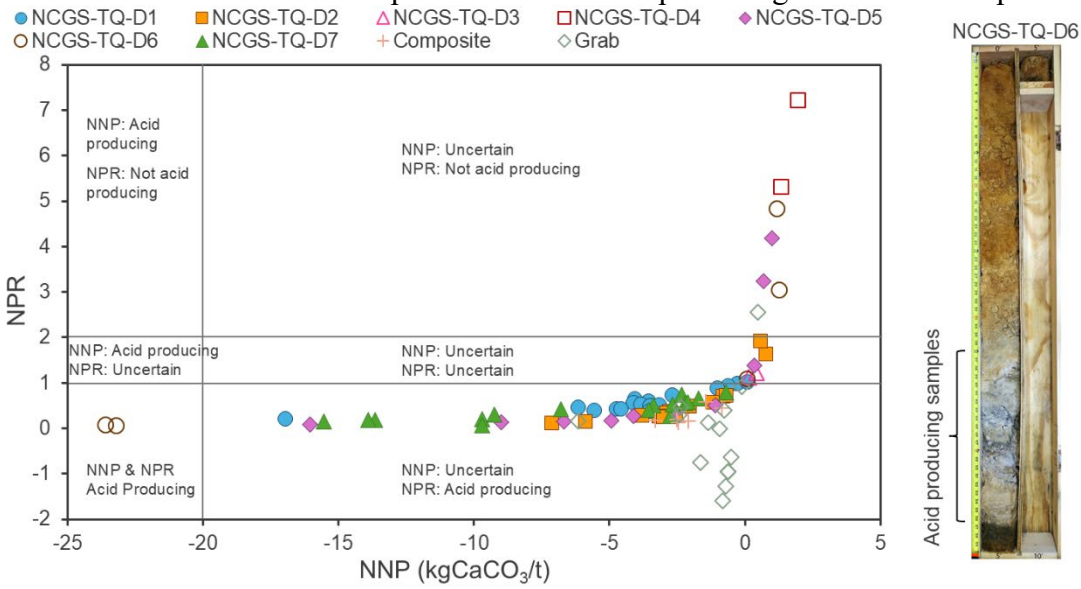

Figure 38. Acid-base accounting data for composite, grab, and cores samples. Photograph shows NCGS-TQ-D6 with acid producing samples noted. See text for details.

amongst the highest in S concentration and have elevated levels of some critical minerals found in sulfides (Figures 32-34). Sulfide minerals are important contributors to acid rock drainage (International Network for Acid Prevention, 2009). Thus, abundant sulfides in these samples likely contribute to their net acid producing potential.

6. Conclusions

The Tungsten Queen tailings have been identified as a probable resource for tungsten and may be a source for additional critical minerals discussed in this report. Determining the economic viability of critical mineral extraction was beyond the scope of this project, however, the dominantly-quartz Tungsten Queen tailings represent an interesting scenario since processing them for high-purity quartz would concentrate the non-quartz, critical mineral-bearing minerals, possibly altering what may be economic to extract.

Lateral and depth-related variability in critical mineral content were observed in the Tungsten Queen tailings impoundment data. Lateral variability may be caused by density and/or

grainsize variations while differences in critical mineral concentration with depth may relate to deposit heterogeneity. Collectively, these observations could have interesting implications for the relationship between grain size, mineral density, vein heterogeneity, and the distribution of critical mineral and non-critical commodity concentrations in the tailings ponds. However, additional research is needed to better constrain what role, if any, each plays.

Differences in the concentration of W with respect to Mn, and S with respect to Sb, As, and Te were observed between tailings ponds 2 and 3. Bivariate diagrams of Mn versus W show clear but different data trends, with tailings from pond 2 showing higher W for a given Mn concentration than those in pond 3, likely resulting primarily from variations in the W and Mn content of hubnerite within the Tungsten Queen vein. The presence of high-Mn, low-W minerals and possible metal leaching could contribute to data scatter, however PCA notes similar behavior for Mn and W, suggesting hubnerite primary controls the concentration of both elements in Tungsten Queen tailings samples. Source heterogeneity in the critical mineral content of some sulfide minerals and variations in sulfide mineral abundances between ponds may partially account for inter-pond variations in Sb, As, and Te versus S. However, the breakdown of certain sulfides, likely by oxidation, may also play a significant role, as supported by PCA results that show Sb, As, and Te with a different principal component than that of S. Thus, the inter-pond variability likely reflects variations in mineral chemistry due to source heterogeneity and/or sulfide oxidation and possible metal leaching, although more research is necessary to determine the influence of each.

This study subtracted a ground-truthed, pre-tailings surface from a LiDAR-derived modern surface to calculate an estimated tailings volume of 43,400,000 ft^3, representing a net 6.7% increase over the estimate of Meyertons (1975). This volume calculation does not include a small body of tailings Meyertons (1975) noted at the base of the Tungsten Mining Corporation mill, now gone and presumed to have been removed by environmental remediation efforts, or tailings that were reportedly pumped into the underground shafts and thus currently inaccessible. The 43,400,000 ft^3 corresponds to 2,706 t W (3,413 t WO_3) contained in the Tungsten Queen tailings pond, which is ~99% lower than Meyertons (1975) estimate for tailings in the impoundment. The lower weighted mean WO_3 calculated by this study causes the discrepancy in the estimates, and could partly be due to this study's inability to access WO_3-rich areas of tailings pond 3 that were sampled by Meyertons (1975). Resource estimates for the 14 critical minerals and non-critical commodities prioritized in this report range from 66,695 t for F to 8 t for Ge.

NNP and NPR values for most Tungsten Queen samples fall within the range of uncertainty for one or both parameters, suggesting kinetic testing may be necessary to more accurately evaluate the potential for net acid production. However, samples NCGS-TQ-D6-3-4 and NCGS-TQ-D6-4-4.7 plot in the net acid producing region for both NNP and NPR like due to an inferred abundance of sulfide minerals which are important contributors to acid rock drainage.

7. References

Abraham, J., 2009, A hydrogeological assessment of arsenic in the Carolina terrane of Union County, North Carolina: Division of Water Resources Groundwater Circular 2009–01, 1–40 p.

Aitchison, J., 1984, The Statistical Analysis of Geochemical Compositions: v. 16, p. 15–18.

Blake, D.E., Stoddard, E.F., Bradley, P.J., Pelt, K.E., 2025, Compiled bedrock geologic map of the Henderson and western portion of the Roanoke Rapids 30' x 60' quadrangles, North Carolina, North Carolina Geological Survey, Open-file Report 2025-04, scale 1:100,000.

Boschetty, F.O., Ferguson, D.J., Cortés, J.A., Morgado, E., Ebmeier, S.K., Morgan, D.J., Romero, J.E., and Silva Parejas, C., 2022, Insights Into Magma Storage Beneath a Frequently Erupting Arc Volcano (Villarrica, Chile) From Unsupervised Machine Learning Analysis of Mineral Compositions: Geochemistry, Geophysics, Geosystems, v. 23, p. 1–24, doi:10.1029/2022GC010333.

Bowman, J.D., 2010, The Aaron Formation: Evidence for a New Lithotectonic Unit in Carolinia, North Central North Carolina [M.S.]: North Carolina State University, 116 p.

Bowman, J.D., Hibbard, J.P., and Miller, B.V., 2013, The Virgilina sequence redefined, north central North Carolina, *in* Hibbard, J.P. and Pollock, J. eds., One Arc, Two Arcs, Old Arc, New Arc, The Carolina Terrane in Central North Carolina, Salisbury, North Carolina, Carolina Geological Society Annual Meeting and Field Trip, p. 127–138.

Bradley, P.J., and Miller, B.V., 2011, New geologic mapping and age constraints in the Hyco Arc of the Carolina terrane in Orange County, North Carolina: Geological Society of America Abstracts with Programs, v. 43.

Casadevall, T., and Rye, R.O., 1980, The Tungsten Queen Deposit, Hamme District, Vance County, North Carolina: A Stable Isotope Study of a Metamorphosed Quartz-Huebnerite Vein: Economic Geology, v. 75, p. 523–537.

Chaumba, J.B., Reid, J.C., and Parker, J.C., 2015, Hamme (Tungsten Queen) Mine Tailings, Vance County, North Carolina: Mineral chemistry of Potentially Recoverable Huebnerite-Wolframite and Sulfide Minerals: Southeastern Geology, v. 51, p. 33–49.

Chayes, F., 1960, On correlation between variables of constant sum: Journal of Geophysical Research, v. 65.

Dinwiddie, E., and Liu, X.-M., 2018, Examining the Geologic Link of Arsenic Contamination in Groundwater in Orange County, North Carolina: Frontiers in Earth Science, v. 6, doi:10.3389/feart.2018.00111.

Espenshade, G.H., 1945, Tungsten Deposits of Vance County North Carolina, and Mecklenburg County, Virginia: Bulletin 948-A, 1–17 p.

Feiss, G., Maybin, A.H., III, Riggs, S.R., and Grosz, A.E., 1991, Mineral Resources of the Carolinas, *in* Horton, J.W., Jr. and Zullo, V.A. eds., The Geology of the Carolinas, The University of Tennessee Press, p. 319–345.

Fey, D.L., 2004, Acid-Base Accounting:, https://pubs.usgs.gov/of/2003/ofr-03-210/Section508/IX_Acid-base_Accounting-508.pdf (accessed December 2024).

Foley, N.K., Jaskula, B., Kimball, B.E., and Schulte, R., 2017, Gallium, *in* Schulte, K.J., DeYoung, J.H., Jr., Seal, R.R., II, and Bradley, D.C. eds., Critical mineral resources of the United States—Economic and environmental geology and prospects for future supply, U.S. Geological Survey Professional Paper 1802, p. H1–H35, doi:10.3133/pp1802H.

Foose, M.P., Slack, J.F., and Casadevall, T., 1980, Textural and Structural Evidence for a Predeformation Hydrothermal Origin of the Tungsten Queen Deposit, Hamme District, North Carolina: Economic Geology, v. 75, p. 515–522.
Foose, M.P., Slack, J.F., and Casadevall, T.J., 1981, Textural and Structural Evidence for a Predeformation Hydrothermal Origin of the Tungsten Queen Deposit, Hamme District, North Carolina - A Reply: Economic Geology, v. 74, p. 980–982.
Foose, M.P. and Slack John F., 1978, Premetamorphic Hydrothermal Origin of the Tungsten Queen Vein, Hamme District, North Carolina, as Indicated by Mineral Textures and Minor Structures: U.S. Geological Survey Open-File Report 78-427, p. 1–34.
Gair, J.E., 1977, Maps and Diagrams Showing Structural Control of the Hamme Tungsten Deposit, Vance County, North Carolina: U.S. Geological Survey Miscellaneous Investigations Series Map I-1009, 1 p.
Gair, J.E., Windolph, J.F., and Wright, N.A., 1975, Preliminary Results of Geochemical Soil Survey, Hamme Tungsten District, North Carolina: Geological Survey Circular 711, p. 1–19.
Gnesda, W.R., Karl, N.A., and Mauk, J.L., 2020, Germanium Deposits in the United States:, doi:10.5066/P9CPYTFN.
Greenacre, M., 2021, Compositional data analysis: Annual Review of Statistics and Its Application, v. 8, p. 271–299, doi:10.1146/annurev-statistics-042720-124436.
Hammarstrom, J.M. et al., 2022, Focus areas for data acquisition for potential domestic resources of 11 critical minerals in the conterminous United States, Hawaii, and Puerto Rico—Aluminum, cobalt, graphite, lithium, niobium, platinum-group elements, rare earth elements, tantalum, tin, titanium, and tungsten: U.S. Geological Survey Open-File Report 2019-1023-B Version 1.1, doi:10.3133/ofr20191023B.
Hibbard, J.P., Stoddard, E.F., Secor, D.T., and Dennis, A.J., 2002, The Carolina Zone: overview of Neoproterozoic to Early Paleozoic peri-Gondwanan terranes along the eastern Flank of the southern Appalachians: Earth-Science Reviews, v. 57, p. 299–339, doi:10.1016/S0012-8252(01)00079-4.
Hibbard, J.P., van Staal, C., Rankin, D., and Williams, H., 2006, Lithotectonic Map of the Appalachian Orogen (South), Canada-United States of America: Geological Survey of Canada Map 02096A.
Hibbard, J.P., Pollock, J., and Bradley, P., 2013, One arc, two arcs, old , new arc: An overview of the Carolina terrane in central North Carolina, *in* Hibbard, J.P. and Pollock, J. eds., One Arc, Two Arcs, Old Arc, New Arc, The Carolina Terrane in Central North Carolina, Salisbury, North Carolina, Carolina Geological Society Annual Meeting and Field Trip, p. 35–61.
Hofstra, A.H. et al., 2021, Deposit Classification Scheme for the Critical Minerals Mapping Initiative Global Geochemical Database: U.S. Geological Survey Open-File Report Open-File Report 2021–1049.
Hofstra, A.H., and Kreiner, D.C., 2020, Mineral Resources Program Systems-Deposits-Commodities-Critical Minerals Table for the Earth Mapping Resources Initiative (ver. 1.1, May 2021): U.S. Geological Survey Open-File Report 2020–1042, p. 26.
Horton, J.W., Jr., Peper, J.D., Burton, W.C., Weems, R.E., and Sacks, P.E., 2022, Geologic map of the South Boston 30’ × 60’ quadrangle, Virginia and North Carolina: U.S. Geological Survey Scientific Investigations Map 3483, doi:10.3133/sim3483.

International Network for Acid Prevention, 2009, Global Acid Rock Drainage Guide: 473 p., http://www.gardguide.com (accessed May 2025).
LeHuray, A.P., 1989, U-Pb and Th-Pb whole rock studies in the southern Appalachian Piedmont: Southeastern Geology: Southeastern Geology, v. 30, 77-94.
Le Maitre, R.W., 1982, Chapter 4 - Linear Relationships Between Two Variables, *in* LE MAITRE, R.W.B.T.-D. in P. ed., Numerical Petrology, Elsevier, v. 8, p. 39–57, doi:https://doi.org/10.1016/B978-0-444-42098-5.50008-0.
Meyertons, R., 1975, A Preliminary Estimate of Tungsten Content of Tungsten Queen Tailing for Ranchers Exploration & Development Corporation:, 1–11 p.
Mueller, P., Kozuch, M., Heatherington, A., Wooden, J., Offield, T, Koeppen, R., Klein, T., and Nutman, A., 1996, Evidence for Mesoproterozoic basement in the Carolina terrane and speculation on its origins, *in* Nance, D. and Thompson, M. eds., Avalonian and Related Peri-Gondwanan Terranes of the Circum-North Atlantica, Geological Society of America Special Paper 304, p. 207–217.
Nassar, N.T., Shojaeddini, E., Alonso, E., Jaskula, B., and Tolcin, A., 2024, Quantifying potential effects of China's gallium and germanium export restrictions on the U.S. economy: U.S. Geological Survey Open-File Report 2024–1057, doi:10.3133/ofr20241057.
North Carolina Department of Natural and Cultural Resources, 2023, Tungsten Queen (G-139):, https://www.dncr.nc.gov/blog/2023/12/20/tungsten-queen-g-139#:~:text=Haile%20expanded%20the%20Vance%20County,Exploration%20Company%20acquired%20the%20property (accessed May 2025).
Parker, J.M., 1963, Geologic Setting of the Hamme Tungsten District, North Carolina and Virginia: U.S. Geological Survey Bulletin 1122-G, 1–66 p., doi:10.3133/b1122G.
Parker, J.C., Reid, J.C., and Chaumba, J.B., 2015, Hamme (Tungsten Queen) Mine Tailings, Vance County, North Carolina: Mineral Chemistry of Potentially Recoverable Huebernite-Wolframite and Sulfide Minerals: Geological Society of America Abstracts with Programs, v. 47, p. 6.
Pawlowsky-Glahn, V., Egozcue, J.J., and Tolosana-Delgado, R., 2015, Modeling and Analysis of Compositional Data: 1–247 p., doi:10.1002/9781119003144.
R Core Team, 2022, R: A Language and Environment for Statistical Computing: Vienna, R Foundation for Statistical Computing.
Reid, J.C., Taylor, K.B., Mensah-Biney, R., Simms, J., and Akbari, H., 2017, Tungsten Queen Mine Tailings Evaluation, Vance Co., NC: A Potential Silica Resource: North Carolina Geological Survey Open-file report, v. 2017–01, p. 1.
Secor, D.T., Samson, S.L., Snoke, A.W., and Palmer, A.R., 1983, Confirmation of the Carolina Slate Belt as an Exotic Terrane: Science, v. 221, p. 649–651, doi:10.1126/science.221.4611.649.
Skousen, J., Simmons, J., and Ziemkiewicz, P., 2001, The Use of Acid-Base Accounting to Predict Post-mining Drainage Quality On West Virginia Surface Mines: Reclamation Sciences, v. 1, doi:10.21000/JASMR01010437.
U.S. Army Corps of Engineers, 2017, Draft Environmental Assessment Use of Borrow Areas for Island Creek Dam Repair John H. Kerr Dam and Reservoir, Mecklenburg County, Virginia:, 1–22 p.
U.S. Department of Interior Bureau of Mines, 1944, War Minerals Report: Regional File No. E-453-A, 1–67 p.

U.S. Environmental Protection Agency, 1994, Acid Mine Drainage Prediction: U.S. Environmental Protection Agency Special Waste Branch Technical Document EPA 530-R-94-036, 48 p., https://www.epa.gov/sites/default/files/2015-09/documents/amd.pdf (accessed June 2025).

U.S. Geological Survey, 2022, 2022 Final List of Critical Minerals:, https://d9-wret.s3.us-west-2.amazonaws.com/assets/palladium/production/s3fs-public/media/files/2022%20Final%20List%20of%20Critical%20Minerals%20Federal%20Register%20Notice_2222022-F.pdf (accessed April 2024).

U.S. Geological Survey, 2023, USGS protocols for sampling mine waste in support of Earth MRI:

White, W.A., 1943, Tungsten Deposit Near Townsville, North Carolina (Advance Report): North Carolina Department of Conservation and Development Division of Mineral Resources Mineral Investigation I.

Wortman, G.L., Sampson, S.D., and Hibbard, J.P., 2000, Precise U-Pb zircon constraints on the earliest magmatic history of the Carolina terrane: Journal of Geology, v. 108, p. 321–338.

8. Appendices

Note: Appendices can be downloaded from the North Carolina Geological Survey website.

Appendix 1
Tungsten Queen Field Sheets

Appendix 2
Tungsten Queen Sonic Core Photos

Appendix 3
Tungsten Queen Geochemical Data

Appendix 4
Tungsten Queen PCA data

9. Terms of Use for NCGS Products

The use of information contained within ***Critical Mineral Characterization of the Tungsten Queen Mine Tailings, Vance County, North Carolina***, as well as the additional data contained within the appendices, is encouraged for any persons or entities, with emphasis on industry professionals, county and municipal governments, and other state government agencies working within North Carolina. As part of our mission states, the NCGS examines, surveys, and maps the geology, mineral resources, and topography of the state to encourage the wise conservation and use of these resources by industry, commerce, agriculture, and government agencies for the general welfare of the citizens of North Carolina. The NCGS conducts basic and applied research projects in environmental geology, mineral resource exploration, hazards mapping, and systematic geologic mapping. Services include identifying rock and mineral samples submitted by citizens and providing consulting services and specially prepared reports to agencies that require geological information. In addition to digital means of distribution, via interactive web-map products, the Geological Survey Section publishes Bulletins, Information Circulars, Open-file Reports and Maps, Field Trip Guidebooks, Geologic Map Series, and Special Publications, all of which can be requested from the NCGS publications ordering page.

10. Acknowledgement

Townsville Timber, Inc. for their project support and access permission to the Tungsten Queen mine site.
United States Tungsten, Inc. for their cooperative discussions and support throughout the project.
Cascade Drilling Services, for their help with recovering drill core from the site.
U.S. Geological Survey, for funding grant G23AC00423.